

Division of Engineering Research on Call Agreement #34652

Task 1 – Strength Reduction Method (SRM) Evaluation

Peter Narsavage, Daniel Pradel

for the Ohio Department of Transportation
Office of Statewide Planning and Research

and the
United States Department of Transportation
Federal Highway Administration

July 2021

Final Report



E.L. Robinson Engineering of Ohio



The Ohio State University

1. Report No. FHWA-OH/2021-23	2. Government Accession No.	3. Recipient's Catalog No.	
4. Title and Subtitle Division of Engineering Services Research On-Call Agreement #34652 Task #1 Strength Reduction Method (SRM) Evaluation		5. Report Date July 2021	
		6. Performing Organization Code	
7. Author(s) Peter Narsavage (ORCID 0000-0002-1823-9402) Daniel Pradel (ORCID 0000-0002-9925-1082)		8. Performing Organization Report No.	
9. Performing Organization Name and Address E.L. Robinson Engineering of Ohio Company 950 Goodale Boulevard, Suite 180 Grandview Heights OH 43212 and The Ohio State University 281 W. Lane Ave. Columbus, OH 43210		10. Work Unit No. (TRAIS)	
		11. Contract or Grant No. State Job No. 34652 Agreement # 34652	
12. Sponsoring Agency Name and Address Ohio Department of Transportation Office of Statewide Planning and Research 1980 West Broad St. Columbus, OH 43223		13. Type of Report and Period Covered Final Report	
		14. Sponsoring Agency Code	
15. Supplementary Notes Prepared in cooperation with the Ohio Department of Transportation (ODOT) and the U.S. Department of Transportation, Federal Highway Administration			
16. Abstract The Ohio Department of Transportation (ODOT) wishes to compare their current industry standard landslide stabilization analysis method using traditional Limit Equilibrium Methods (LEM) to the Strength Reduction Method (SRM) of stability analysis, by reanalyzing two landslide projects with various SRM and LEM software packages and comparing the results. The SRM is described and compared to the LEM, and ODOT's method of designing landslide stabilization piles (Geotechnical Bulletin 7) is explained. The results indicate that the safety factors from SRM compare well with Spencer and Morgenstern-Price methods of LE analysis for unreinforced slopes. For the slope reinforced with a stabilization pile, the SRM analysis was limited by the safety factor of the slope below the pile. Consequently, a direct comparison of maximum bending moment between SRM and GB 7 could not be made. But when the maximum bending moment in the pile was normalized by the change in safety factor from the unreinforced slope to the reinforced slope, the bending moment prediction from the SRM and GB 7 were very similar. The SRM is recommended when analyzing a slope with more than one row of piles. Either GB 7 or SRM may be used for a single row of piles, but both have different limitations. When the slope is not reinforced with piles, LEM and SRM should provide similar results. When subsurface conditions are complex, the use of SRM is beneficial to ensure the LEM search did not miss the critical non-circular failure surface.			
17. Key Words		18. Distribution Statement No Restrictions. This document is available to the public through the National Technical Information Service, Springfield, Virginia 22161	
19. Security Classif. (of this report) Unclassified	20. Security Classif. (of this page) Unclassified	21. No. of Pages	22. Price

SI* (MODERN METRIC) CONVERSION FACTORS

APPROXIMATE CONVERSIONS TO SI UNITS		APPROXIMATE CONVERSIONS FROM SI UNITS	
Symbol	When You Know	When You Know	Symbol
Multiply By		Multiply By	
To Find		To Find	
LENGTH			
in	inches	mm	millimeters
ft	feet	m	meters
yd	yards	m	meters
mi	miles	km	kilometers
AREA			
in ²	square inches	mm ²	square millimeters
ft ²	square feet	m ²	square meters
yd ²	square yards	m ²	square meters
ac	acres	ha	hectares
mi ²	square miles	km ²	square kilometers
VOLUME			
fl oz	fluid ounces	mL	milliliters
gal	gallons	L	liters
ft ³	cubic feet	m ³	cubic meters
yd ³	cubic yards	m ³	cubic meters
NOTE: Volumes greater than 1000 L shall be shown in m ³ .			
MASS			
oz	ounces	g	grams
lb	pounds	kg	kilograms
T	short tons (2000 lb)	Mg	megagrams (or "metric ton")
T	short tons (2000 lb)	Mg	megagrams (or "metric ton")
TEMPERATURE (exact)			
°F	Fahrenheit temperature	°C	Celsius temperature
	5(°F-32)/9		Celsius temperature
	or (°F-32)/1.8		temperature
ILLUMINATION			
fc	foot-candles	lx	lux
fl	foot-Lamberts	cd/m ²	candela/m ²
FORCE and PRESSURE or STRESS			
lbf	poundforce	N	newtons
lbf/in ²	poundforce per square inch	kPa	kilopascals
or psi			

* SI is the symbol for the International Symbol of Units. Appropriate rounding should be made to comply with Section 4 of ASTM E380. (Revised September 1993)

Division of Engineering Research on Call Agreement #34652

Task 1 – Strength Reduction Method (SRM) Evaluation

**Peter Narsavage¹
Daniel Pradel²**

¹E. L. Robinson Engineering of Ohio Company
950 Goodale Boulevard, Suite 180
Grandview Heights, OH 43212

²The Ohio State University
281 W Lane Ave.
Columbus, OH 43210

Prepared in cooperation with the
Ohio Department of Transportation
and the
U.S. Department of Transportation, Federal Highway Administration

The contents of this report reflect the views of the authors who are responsible for the facts and the accuracy of the data presented herein. The contents do not necessarily reflect the official views or policies of the Ohio Department of Transportation or the Federal Highway Administration. This report does not constitute a standard, specification or regulation.

Final Report

July 2021

Division of Engineering Research on Call Agreement #34652

Task 1 – Strength Reduction Method (SRM) Evaluation

Peter Narsavage, M.S., P.E.

E.L. Robinson Engineering of Ohio
950 Goodale Boulevard, Suite 180
Grandview Heights, OH 43212



Daniel Pradel, Ph.D., P.E.

The Ohio State University
281 W Lane Ave.
Columbus, OH 43210



July 2021



Credits and Acknowledgments

Prepared in cooperation with the Ohio Department of Transportation
and the U.S. Department of Transportation, Federal Highway Administration

The contents of this report reflect the views of the author(s) who is (are) responsible for the facts and the accuracy of the data presented herein. The contents do not necessarily reflect the official views or policies of the Ohio Department of Transportation or the Federal Highway Administration. This report does not constitute a standard, specification, or regulation.

The authors thank Louis Schulte, Dora de Mello, and Isaac Kreitzer for their assistance in the analyses. We also thank Kevin White for his review and recommendations for the report and for performing as the Research-on-Call Project Manager.

The research team thanks the Ohio Department of Transportation for their sponsorship of this project. We specifically note the contribution of the Technical Advisory Committee members: Messrs. Christopher Merklin, Stephen Taliaferro, and Andrew Chudzik. Their guidance throughout the project was instrumental for the success of the research. The research team also thanks Ms. Michelle Lucas of the Office of Statewide Planning and Research for her time and assistance.

Table of Contents

List of Tables	ii
List of Figures	ii
1 Introduction.....	1
1.1 Scope of Work	1
1.2 Outline of the Report	1
2 Strength Reduction Method (SRM)	2
2.1 Description of SRM	2
2.2 Comparison of Results to Limit Equilibrium	3
2.3 Application of the Strength Reduction Method	3
2.4 Benefits of the Strength Reduction Method	6
2.5 Effect of Structural Elements on the Critical Failure Surface	8
2.6 Arching Between Piles.....	9
2.7 Finite Element (FE) and Finite Difference (FD) Method Formulations.....	13
2.8 Software Programs for SRM Analyses.....	15
2.8.1 FLAC/Slope	15
2.8.2 FLAC	15
2.8.3 RS2.....	16
2.8.4 Sigma/W	16
3 Design of Landslide Stabilization Piles Using LEM (GB 7)	16
4 Comparison of Analyses Results	18
4.1 Slope without Stabilization Piles, OTT-2-27.18.....	18
4.2 Slope with Stabilization Piles, MUS-16-6.70.....	25
5 Recommendations for SRM.....	31
5.1 When to use SRM.....	31
5.2 Soil Model and Soil Properties	31
5.3 Soil-Structure Interaction (spring models used to connect soil and pile meshes)	32
5.4 General Recommendations for SRM.....	33
6 References.....	34

List of Tables

Table 1 – Safety Factor for Slope at OTT-2-27.18	19
Table 2 – Safety Factor for Slope at MUS-16-6.70	26
Table 3 – Stabilization Pile Results	26

List of Figures

Figure 1 – Elasto-plastic model used in the SRM.....	2
Figure 2 – Accuracy of slope stability methods according to Duncan (1996).....	3
Figure 3 – Application of the SRM to the MUS-16 cross-section. a) critical failure mode predicted by FLAC; b) maximum displacement vs. strength reduction factor.....	4
Figure 4 – Stability analyses for the slope below the piles of the MUS-16 cross-section.....	5
Figure 5 – Diagrams showing the influence of the bending capacity of piles on the position of the critical failure surface for piles near the toe of the slope.....	7
Figure 6 – Diagrams showing the influence of the bending capacity of piles on the position of the critical failure surface for piles near the top of the slope.....	8
Figure 7 – Using piles result in a modification of the critical failure surface in both traditional analyses using: a) the method of slices analyses, and b) FLAC.	10
Figure 8 – Diagrams showing the influence of the bending capacity of piles on the position of the critical failure surface and loading received by the piles.....	11
Figure 9 – Spring characteristics needed to model the interaction between piles and soils.	12
Figure 10 – Pushover analysis of a pile performed in FLAC to obtain its lateral force vs displacement relation (p – y type curve).....	13
Figure 11 – First three iterations in the solution of a non-linear problem converging at large shear strains towards a shear stress $\tau = \tau_r$	14
Figure 12 – OTT-2 Digout Drained Conditions, Shear Strain from FLAC/Slope (top) and total displacements from RS2 (bottom)	21
Figure 13 – Vector Norm Displacements for OTT-2 from Sigma/W Left - ex. conditions, w/o residual; Right digout, drained conditions	22
Figure 14 – Unbalanced Energy and Domain Stiffness for OTT-2 ex. conditions, w/o residual from Sigma/W.....	22
Figure 15 – Unbalanced Energy and Domain Stiffness for OTT-2 digout, drained conditions from Sigma/W.....	23
Figure 16 – SRM Convergence Plots for OTT-2 ex. conditions, w/o residual from RS2.....	23
Figure 17 – SRM Convergence Plots for OTT-2 ex. conditions, with residual from RS2.....	24
Figure 18 – SRM Convergence Plots for OTT-2 digout undrained conditions from RS2	24
Figure 19 – SRM Convergence Plots for OTT-2 digout drained conditions from RS2	25
Figure 20 – MUS-16 Existing Conditions, Displacements from RS2 (top) and FLAC/Slope (bottom).....	27
Figure 21 – MUS-16 Convergence Plot from RS2.....	28
Figure 22 – Unbalanced energy, Domain Stiffness, and Vector Norm Displacement for MUS-16 for ex. conditions from Sigma/W.....	29
Figure 23 – Determination of Reasonable Maximum Bending Moment for MUS-16 using FLAC.	30
Figure 24 – Local slope instability in an area away from the slope being stabilized	33

1 Introduction

1.1 Scope of Work

The Ohio Department of Transportation (ODOT) wishes to compare their current industry standard landslide stabilization analysis method using traditional Limit Equilibrium Methods (LEM) to the Strength Reduction Method (SRM) which uses Finite Element (FE) or Finite Difference (FD) numerical modeling techniques. The scope is to reanalyze two landslide projects, OTT-2-27.18 (PID 107104) and MUS-16-6.70 (PID 113521) and compare SRM results with LEM analyses. For the MUS-16 project, the research team also compared the analysis process described in Geotechnical Bulletin 7 (GB 7) (ODOT, 2020) for the design of landslide stabilization drilled shafts.

The project goals are:

1. Compare the LEM in GB 7 to the SRM for the design of drilled shaft landslide stabilization.
2. Compare analysis using LEM for an earthwork solution to the SRM of analysis.
3. Determine when SRM should be considered in preference to LEM slope stability and drilled shaft stabilization design.
4. Provide recommendations for soil models, soil properties, and spring models used to connect soil and pile meshes.
5. Explain the process, benefits, and differences that numerical modeling has to offer.

1.2 Outline of the Report

Chapter 2 describes the SRM and discusses how it compares to LEM, the application of SRM, its benefits and important considerations. Chapter 2 also discusses the software programs included in this study.

Chapter 3 describes the design procedure presented in Geotechnical Bulletin 7 for LEM.

Chapter 4 summarizes a comparison of results between SRM and LEM analyses for two landslide projects, OTT-2 and MUS-16.

Chapter 5 presents recommendations for SRM analyses.

2 Strength Reduction Method (SRM)

2.1 Description of SRM

The use of numerical modelling by the Finite Element (FE) and Finite Difference (FD) Methods for slope stability analysis became practical after the introduction of the Strength Reduction Method (SRM) by Griffiths and Lane (1999). The SRM involves modelling subsurface materials as elastic-perfectly-plastic materials, while simultaneously reducing strengths by a strength reduction factor, R (Figure 1). The SRM is generally used in combination with the Mohr-Coulomb failure criterion¹, but the method imposes no restriction as to the strength model and can be used with other models, such as the Hoek-Brown failure criterion commonly used in rock mechanics. When using the Mohr-Coulomb failure criterion the cohesion, c , and friction angle, ϕ , are reduced simultaneously as follows:

$$c_d = \frac{c}{R} \quad [1]$$

$$\tan(\phi_d) = \frac{\tan(\phi)}{R} \quad [2]$$

The reduction in strength in the SRM is repeated iteratively until equilibrium is no longer satisfied and the slope fails in a quasi-natural manner. The highest value of the strength reduction factor, R_{max} , that satisfies equilibrium and is also kinematically acceptable is equivalent to the Factor of Safety, FOS , of the slope:

$$FOS = R_{max} \quad [3]$$

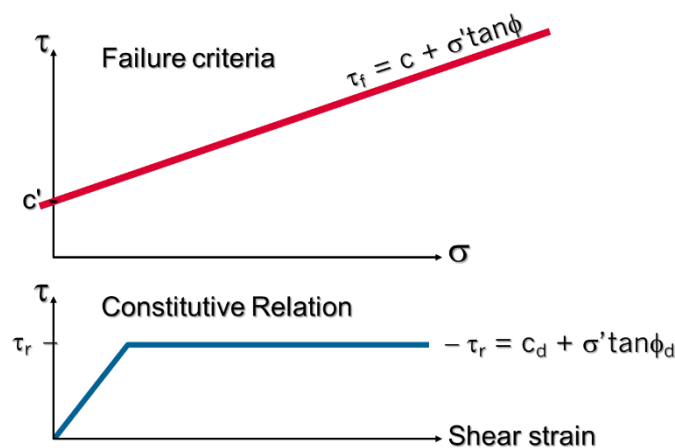


Figure 1 – Elasto-plastic model used in the SRM

¹ Generally written as: $\tau_f = c + \sigma' \tan \phi$ (where c is the cohesion, ϕ is the friction angle, τ_f is the shear stress at failure and σ' is normal stress).

2.2 Comparison of Results to Limit Equilibrium

For methods that satisfy both force and moment conditions of equilibrium (e.g., Bishop for circular surfaces, Spencer and Morgenstern-Price for failures of all shapes) the accuracy of the method of slices is generally considered to be about ± 6 percent according to Duncan's State of the Art, shown in Figure 2 (Duncan J. M., 1996). Publications by the authors of the SRM, have repeatedly shown the excellent agreement between predictions by the SRM and those obtained by traditional methods, such as the Taylor friction circle method. One of the authors of this report (Pradel) has been using the SRM for 15+ years and in his experience, the FOS predicted by the SRM for unreinforced slopes (i.e., R_{max} in Equation [3]) have always fallen within ± 2 percent of analyses results using the Spencer method; hence, there is ample evidence that SRM predictions compare well with traditional slope stability, especially FOS obtained by stringent formulations such as the Morgenstern-Price and Spencer methods. Furthermore, the uncertainty of the different methods is considerably less than the uncertainty with which shear strength or groundwater pressures are determined.

The crux of the issue with regard to evaluating the computational accuracy of the methods is: What is the correct answer to which other answers should be compared? Although it has proven difficult to find absolutely correct answers, it is possible to decide what is the correct answer with sufficient accuracy for all practical purposes. This conclusion is based on the finding that accurate methods of slices give essentially the same values of F as do friction circle analyses, log spiral analyses, and finite-element analyses, all of which involve different approaches to solution of the equilibrium problem. The maximum difference between factors of safety calculated by methods that satisfy all conditions of equilibrium is about 12%, usually less. Thus, with an accuracy of about $\pm 6\%$, factors of safety calculated using methods that satisfy all conditions of equilibrium can be considered to be the correct answer. This is certainly close enough for practical purposes, because slope geometry, water pressures, unit weights and shear strengths can seldom, if ever, be defined with an accuracy as good as $\pm 6\%$.

Figure 2 – Accuracy of slope stability methods according to Duncan (1996)

2.3 Application of the Strength Reduction Method

The aim of the SRM is to find the threshold between stability and instability; i.e., when equilibrium becomes problematic and, as a result, predicted displacements increase exponentially. The corresponding FOS (R_{max} in Equation [3]) can be determined numerically using displacements, energy, or stiffness considerations; one of the best manners to visualize the effect of reducing strength is by plotting the maximum predicted displacement in the FE or FD numerical model versus the strength reduction factor, R , as shown in Figure 3b for the MUS-16 cross-section. For this section, Figure 3a shows that the critical failure mechanism of the slope, is a failure located

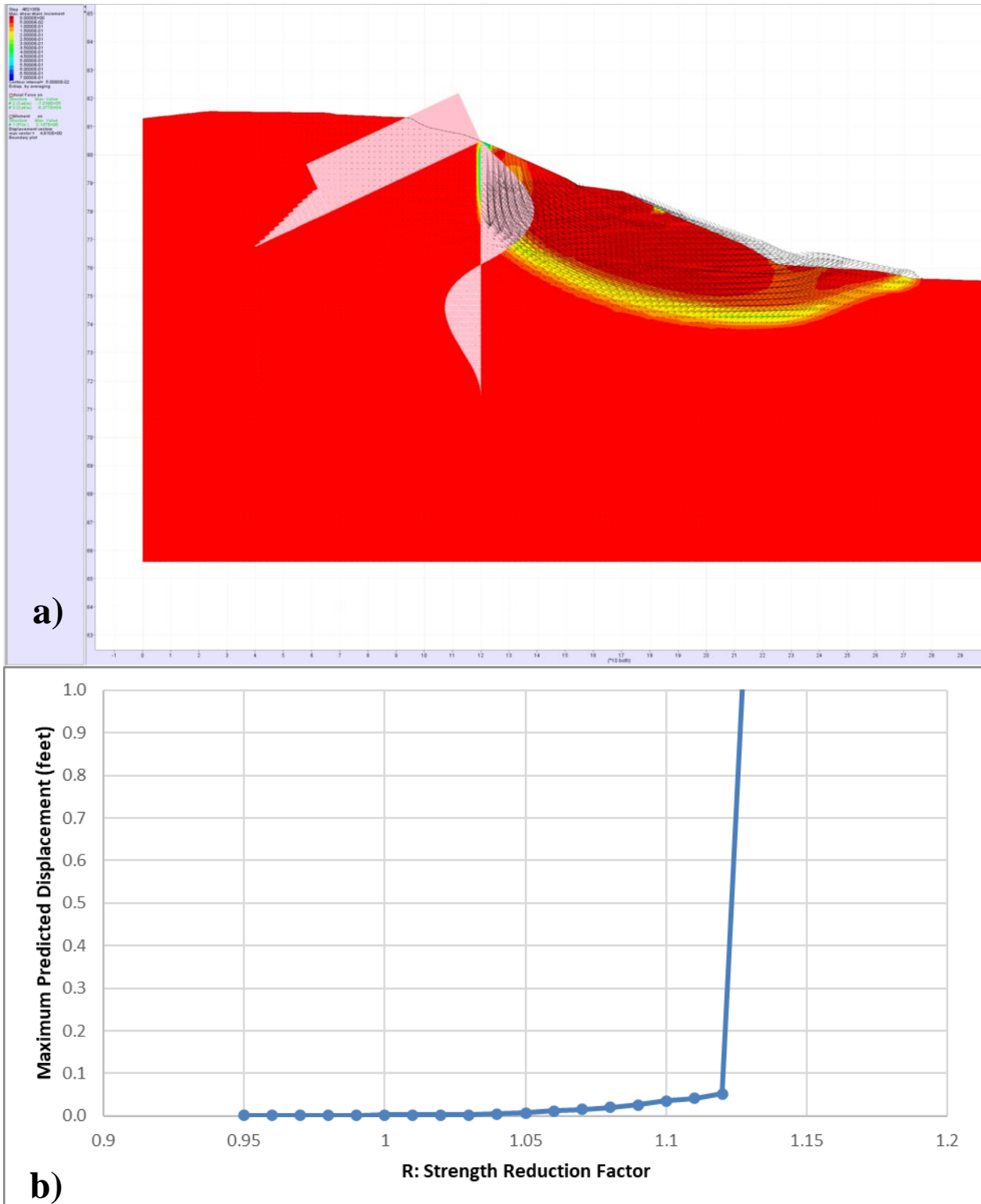


Figure 3 – Application of the SRM to the MUS-16 cross-section. a) critical failure mode predicted by FLAC; b) maximum displacement vs. strength reduction factor.

immediately below the row of stabilizing piles. Structurally, movement of the piles' subjacent slope results in significantly reduced lateral resistance for the piles up to a depth of about 30-feet, as the strength reduction factor approaches $R_{max}=1.12$.

Note that the method of slices predicts a similarly low FOS (about 1.17 by the Spencer and Morgenstern-Price methods) for the slope located immediately downslope of the piles (Figure 4), confirming that a failure of the slope below the piles is critical.

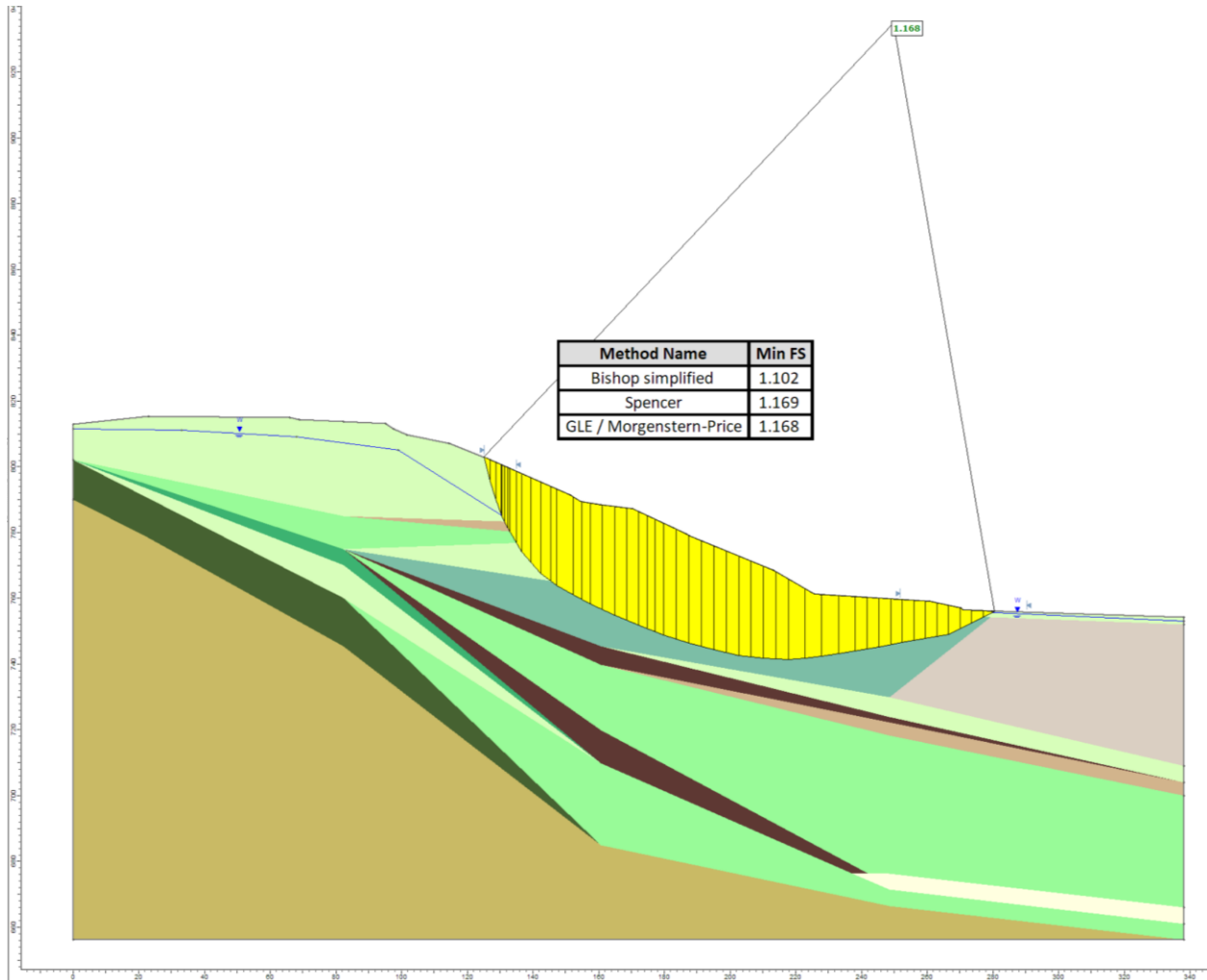


Figure 4 – Stability analyses for the slope below the piles of the MUS-16 cross-section.

As the strength reduction factor approaches $R_{max}=1.13$, the slope movement depicted in Figure 3a, eliminates a significant portion of the passive earth resistance that the slope previously provided to the stabilizing piles. For $R > R_{max}$, predictions of bending moments and ground anchor loads are not meaningful since the slope has already moved away from the piles and is not providing passive resistance. Hence, meaningful predictions of stresses and lateral pressures on structures by the SRM are limited to strength reduction factors up to the factor of safety of the slope (i.e., $R \leq R_{max}$). When using the unbalanced force method, traditional LEMs ignore the effect of other more critical

failure mechanisms and will provide pile loads for factors of safety greater than R_{\max} . For example, one may obtain the lateral pile load for FOS=1.5 using the LEM procedures even though the critical FOS is 1.13 for the slope below the piles. In this situation, the slope below the pile experiences accelerations and moves as the strength is reduced beyond FOS=1.13; thus, the slope below the piles cannot provide the horizontal interslice forces assumed by the LEM analysis for FOS=1.5, and the design of piles for the large lateral load associated with FOS=1.5 is not considered reasonable, nor economical.

2.4 Benefits of the Strength Reduction Method

Perceived advantages of the SRM include:

1. No assumptions (or guesses) about the location and shape of the critical failure surface are required; therefore, the designer does not need to characterize the shape of the failure surface as circular, noncircular or convex, nor to specify the initiation and exit points of potential failures.
2. Predicted critical failure mechanisms are self-evident. For landslide stabilizations this is especially important since the critical failure mechanism may be influenced by the location of several structural elements, as shown in Figure 3a.
3. Structural demands (e.g., bending moments and shear forces for piles, and axial forces in soil nails and ground anchors) are computed as part of the solution and available to the design team, as shown in Figures 3a, 5 and 6.
4. Structural capacities (e.g., yield moment for piles, and ultimate axial load in soil nails and ground anchors) can be specified and their effect on the critical failure mechanism determined, as shown in Figure 5b and Figure 6b.
5. Restrictive hypotheses about interslice forces direction, location or magnitude are not needed, such as the constant thrust force angle hypothesis required in the Spencer Method or the half-sine interslice force distribution often used with the Morgenstern-Price Method.
6. When SRM predictions have been obtained for probable, optimistic and pessimistic design scenarios and construction is closely monitored with surveys and/or instrumentation, the results of the SRM scenarios may be used to evaluate if the adopted soil parameters are appropriate and realistic and may be used to assess the safety of specific construction stages.
7. The mesh used for the SRM can be modified and subjected to earthquake time-histories for assessments of the slope's seismic performance.
8. Modern FE/FD tools often permit batch runs where solutions can be obtained for multiple pile locations, pile lengths, and/or structural properties; thus, numerical models can be used for optimization purposes (Pradel, Garner, & Kwok, 2010).

Figures 3, 5 and 6 illustrate several of the advantages described above. For example, Figure 3a depicts a critical failure surface that is not only non-circular, but also has a complex (not convex) curvature around the toe. Figure 5a depicts a prediction using the SRM for a slope reinforced with

a row of piles placed near the toe of a slope; because the upper slope is unsupported and the pile is modeled as elastic (no yield moment was specified) the critical failure surface develops above the pile and occurs entirely within the slope materials. Note that in both examples (Figure 3a and 5a), the failure modes are evident, and pile bending moments are predicted without any additional assumption or hypothesis; thus, illustrating benefits 1 to 3 listed above. For designers, one added benefit of the SRM is that it provides pile demands even when the failure surface does not intercept the row of stabilizing piles, i.e., for conditions where piles are only peripherally affected by the critical slope failure mechanism. This is shown in Figures 5a and 6a.

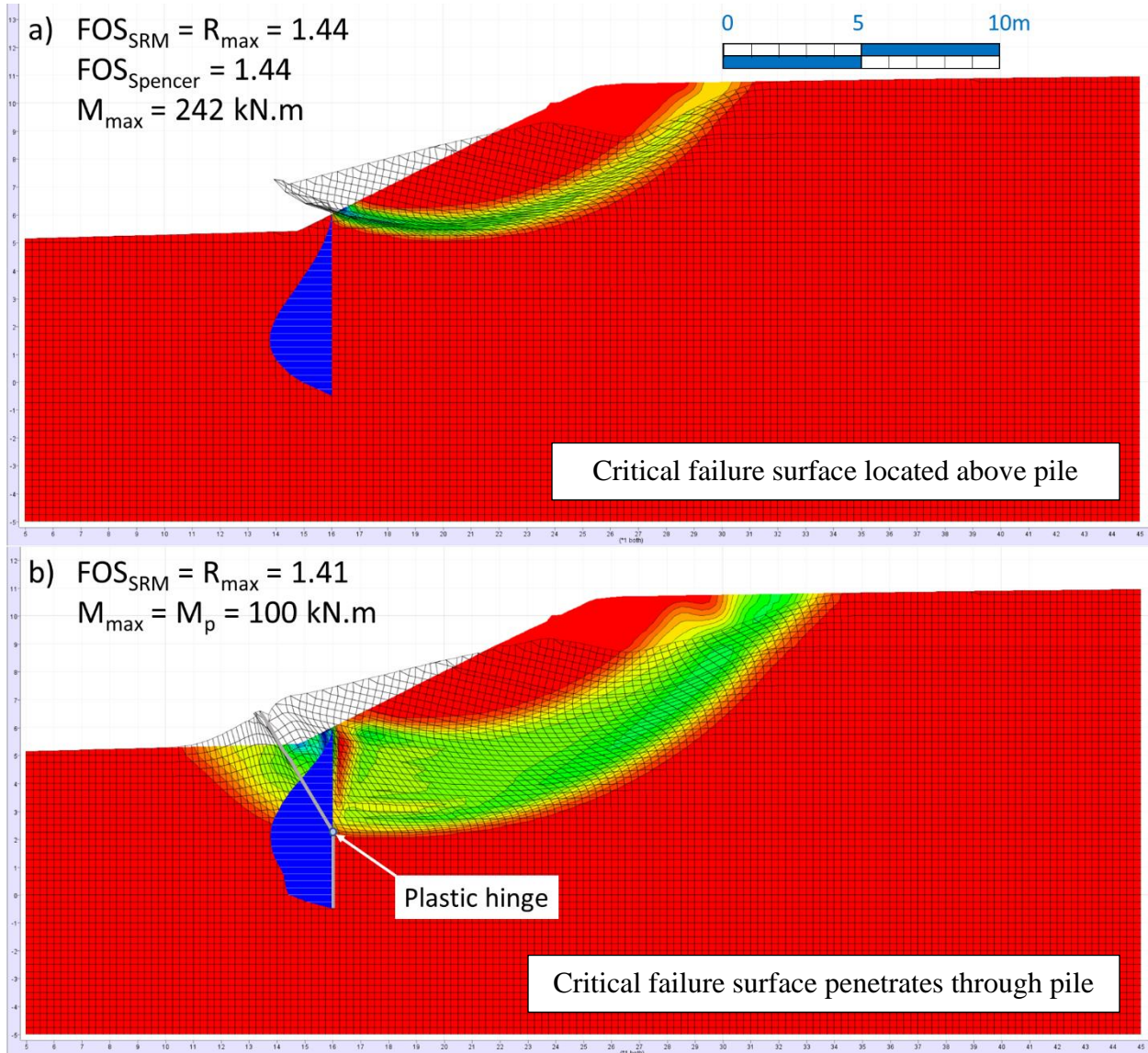


Figure 5 – Diagrams showing the influence of the bending capacity of piles on the position of the critical failure surface for piles near the toe of the slope.

Plots show exaggerated deformed meshes, shear strain contours, and bending moments (blue), predicted using FLAC (Itasca, 2019) for the slope in Poulos (1995) reinforced by a row of piles near the toe of the slope.

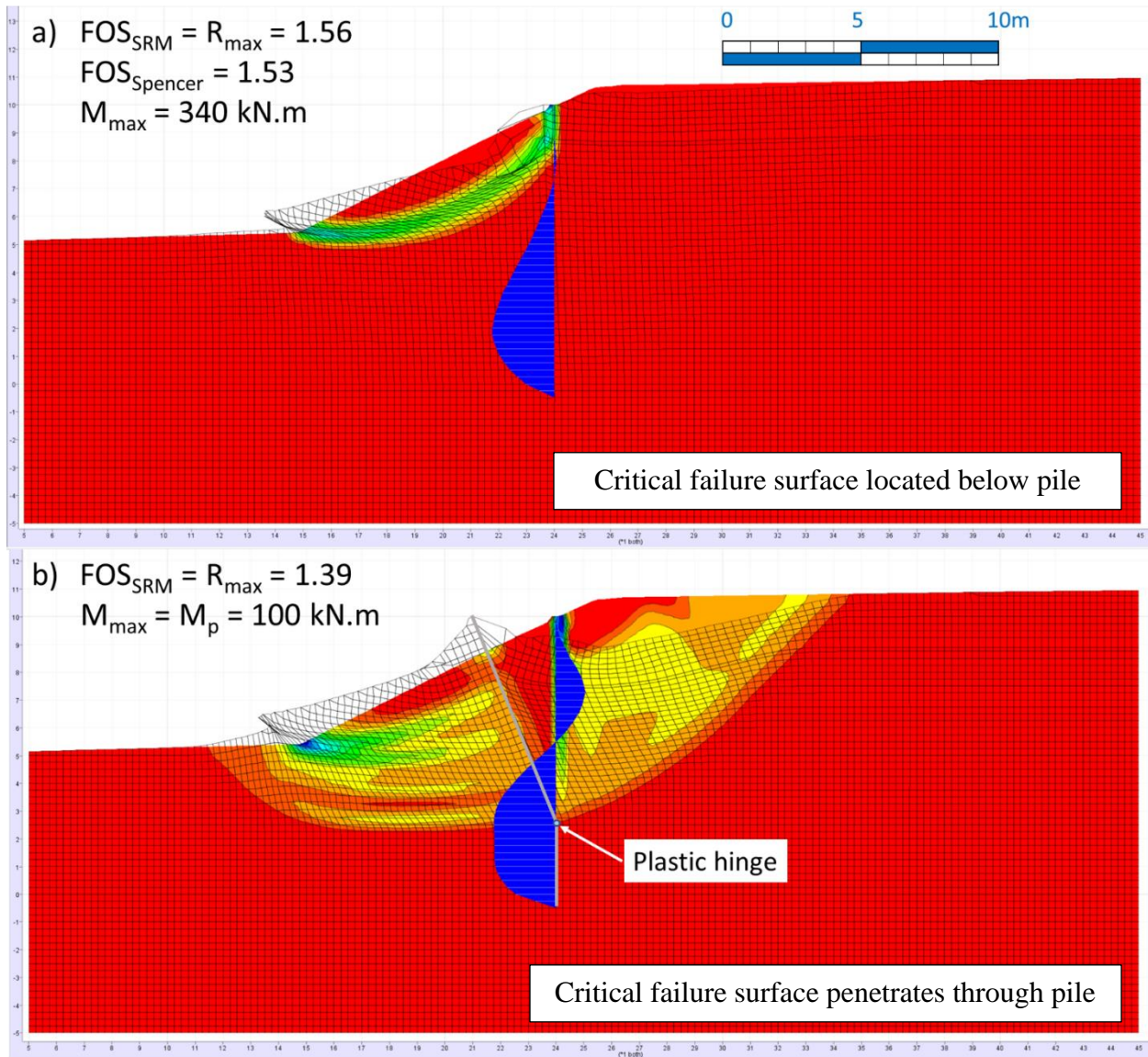


Figure 6 – Diagrams showing the influence of the bending capacity of piles on the position of the critical failure surface for piles near the top of the slope.

Plots show exaggerated deformed meshes, shear strain contours, and bending moments (blue), predicted using FLAC (Itasca, 2019) for the slope in Poulos (1995) reinforced by a row of piles located near the top of the slope.

2.5 Effect of Structural Elements on the Critical Failure Surface

A major issue encountered when using the traditional method of slices is that structural elements modify the shape and location of the critical failure surface. As demonstrated in Yamagami, *et al.* (2000) the large interslice forces created by landslide stabilizing piles commonly results in discontinuous critical basal planes around the pile location in LEM analyses (Figure 7a). Although important, the effect of piles on the position of the critical basal surface is generally ignored by

users of traditional slope stability methods but are often predicted by numerical methods. Note in Figure 7b the discontinuity in high shear zones on both sides of the stabilizing piles.

When multiple structural elements (e.g., several rows of piles) are used, their combined effect on the critical failure plane is more complex, and thus harder to predict. Additionally, because LEMs assume rigid-perfectly plastic movement of the slide mass in the downslope direction, the assumed displacements are generally not kinematically acceptable and the lateral pressure distributions on each structural element cannot be determined uniquely; hence, when multiple rows of piles are present, the individual contribution of each row of piles is undetermined in LEMs. Although the rigid-perfectly plastic kinematics of LEMs are not compatible with beam deflection theory, analyses are commonly performed in practice with LPILE (Ensoft, 2019), using an assumed, or expected, lateral pressure or displacement distribution, for example, as described in NAVFAC (1986), and Hassiotis, Chameau, & Gunaratne (1997). Coming up with a reasonable load or displacement is particularly difficult when several rows of piles and/or ground anchors are present, as shown in Pradel (2018) and Figure 8.

2.6 Arching Between Piles

The interaction between a laterally loaded pile and the surrounding ground is complex and to accurately describe it requires a 3D software program (e.g., FLAC3D or PLAXIS 3D). Because the time necessary to create a 3D mesh is long and analyzing the 3D solution is complex, in practice engineers often use simplified approaches, such as the p-y formulations contained in LPILE (Ensoft, 2019).

Simple guidance on the interaction between laterally loaded piles and the surrounding ground has been reported by a number of sources. For single piles, Broms (1964a and 1964b) assumed a passive resistance of $9 \cdot S_u \cdot D$ for piles in cohesive soils and $3 \cdot K_p \cdot D$ for piles in cohesionless materials (where D is the pile diameter, S_u is the undrained shear strength and K_p is the passive coefficient of earth pressures). Using centrifuge models, Stewart, *et al.* (1994) found that center-to-center spacings of about 5 times the pile diameters were sufficiently large to minimize the interaction between adjacent piles and that flow of soil between piles was fairly certain at spacings of more than 8 diameters. Prakash and Saran (1967) found from load-displacement measurements that the interaction between piles tends to vanish when the center-to-center pile spacing, S , approaches 5 to 6 pile diameters. Hence, for landslide stabilizing piles the literature suggests that full arching conservatively develops when $S \leq 3D$, i.e., when the center-to-center pile spacings is up to 3 pile diameters.

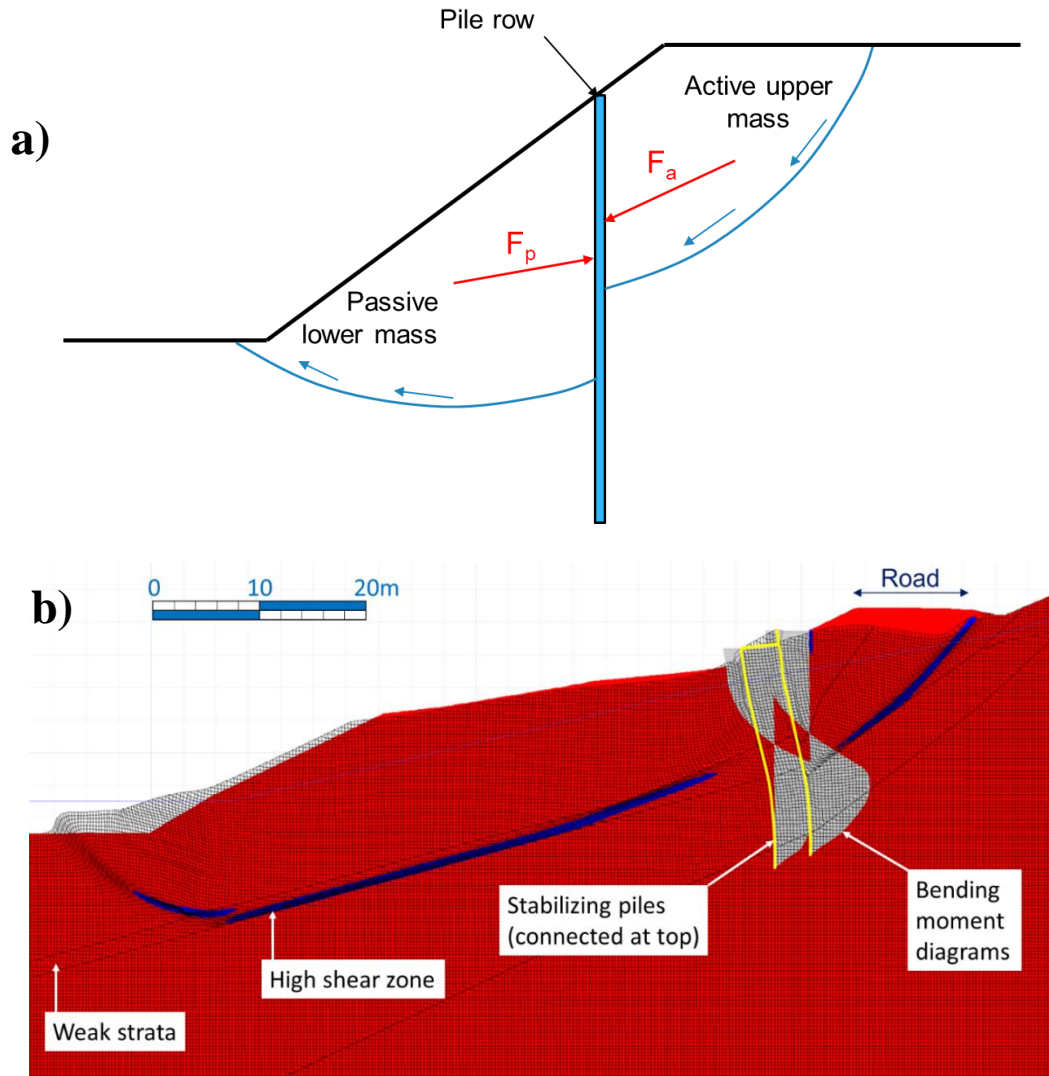


Figure 7 – Using piles result in a modification of the critical failure surface in both traditional analyses using: a) the method of slices analyses, and b) FLAC.

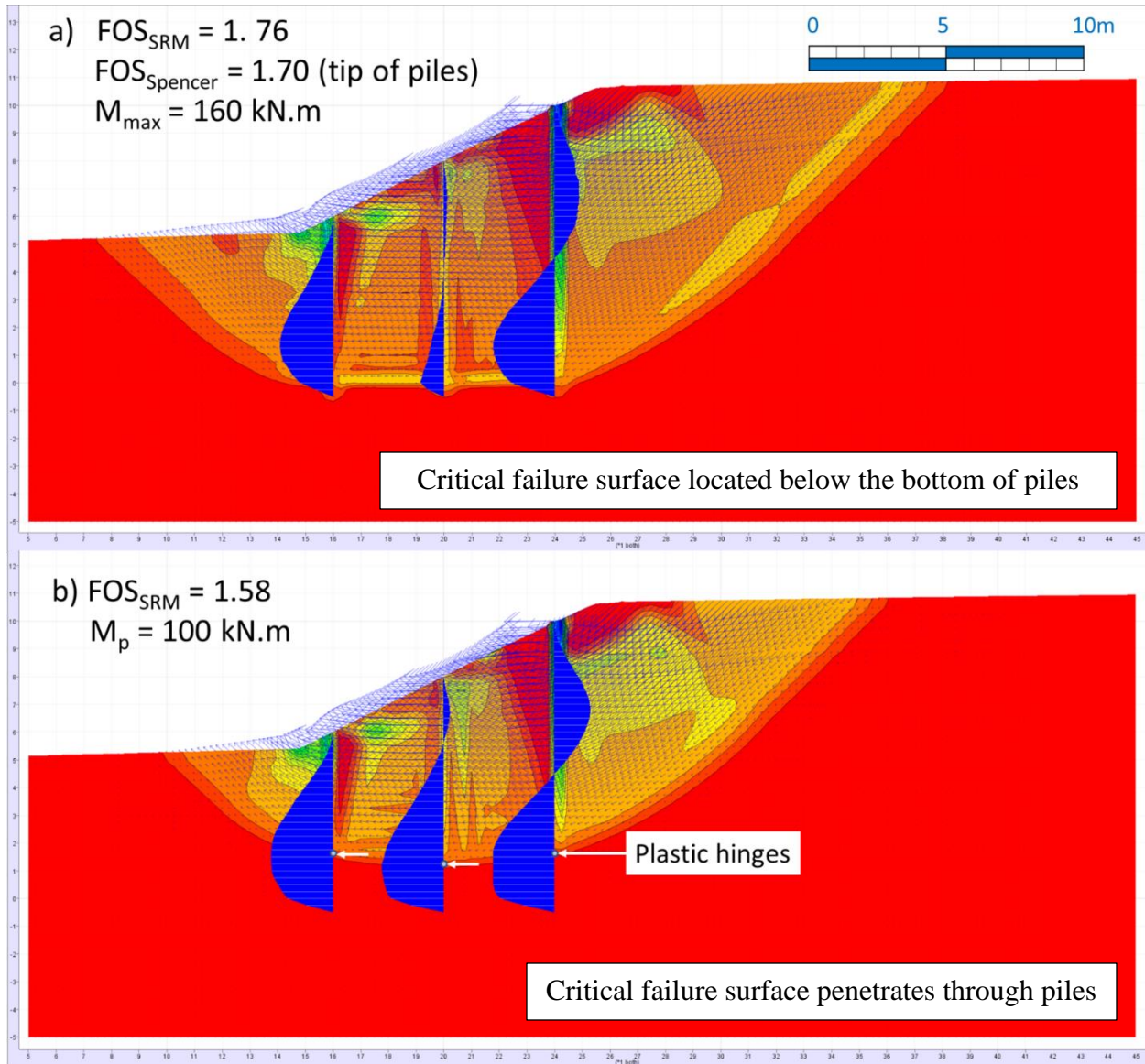


Figure 8 – Diagrams showing the influence of the bending capacity of piles on the position of the critical failure surface and loading received by the piles.
 Plots show exaggerated deformed meshes, shear strain contours, and bending moments (blue), predicted using FLAC (Itasca, 2019) when the slope is reinforced by three rows of piles.

In 2D FE and FD models, multiple non-linear springs are used to connect soil and pile elements; a formulation that allows the soil mesh to move past the piles and simulates the flow of soil between piles when large pile spacings are present. Springs providing lateral resistance may be defined using either:

1. Material appropriate non-linear p-y curves (Figure 9),
2. Simplified bi-linear p-y curves (Figure 9), or alternatively,
3. Pushover analyses performed at multiple depths for different materials (Figure 10).

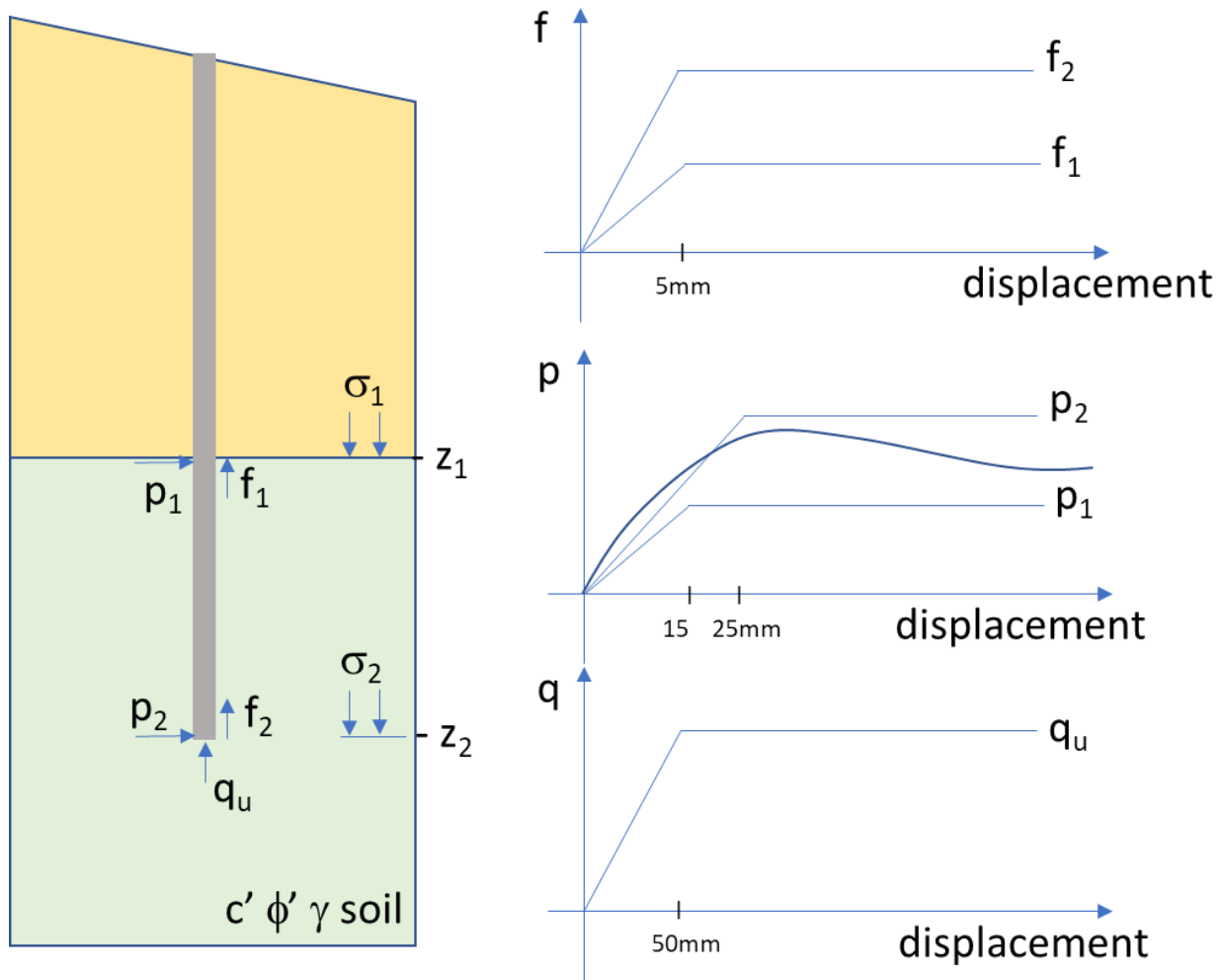


Figure 9 – Spring characteristics needed to model the interaction between piles and soils.
 In the figure threshold displacements (e.g., 5mm) are shown for illustrative purposes only, f_i is the pile skin friction, p_i is the equivalent lateral pressure (as defined in p-y theory), and q_u is the pile's end bearing capacity.

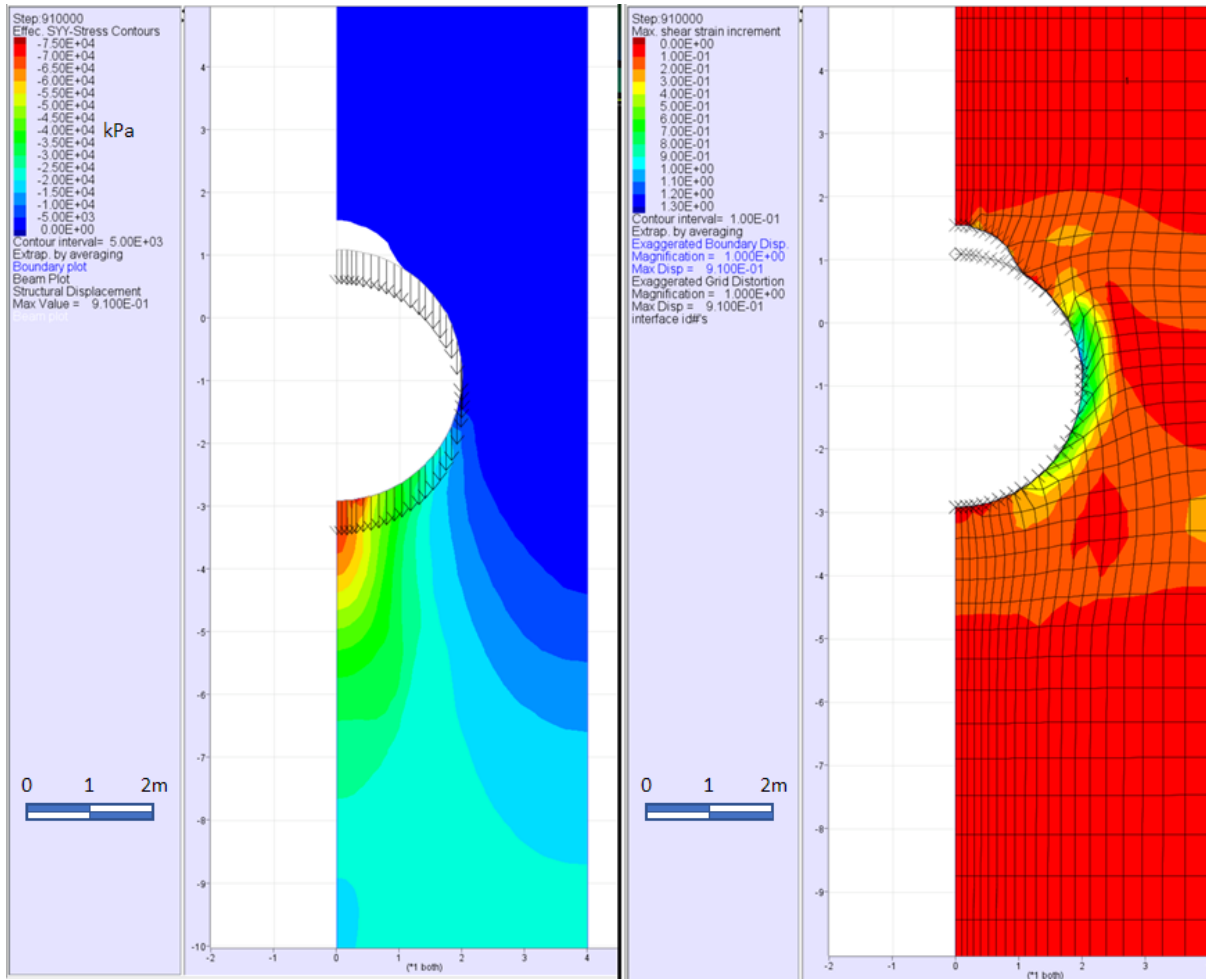


Figure 10 – Pushover analysis of a pile performed in FLAC to obtain its lateral force vs displacement relation (p – y type curve)

2.7 Finite Element (FE) and Finite Difference (FD) Method Formulations

The SRM has been implemented in several FE programs and one FD program commonly used by practicing geotechnical engineers. Because FE and FD programs solve the same equations (equilibrium, geometric compatibility, and stress-strain relations) one would expect all numerical programs to provide identical solutions. In practice that is not necessarily the case and it is worthwhile to examine how solutions are generated to understand why some differences occur. A traditional Finite Element solution is expressed as follows:

$$[SM] \cdot \vec{a} = \vec{F} \quad [4]$$

where:

- $[SM]$ = stiffness matrix
- \vec{a} = vector of nodal displacements
- \vec{F} = resultant force vector (e.g., from gravity, surface loads, etc.)

The formulation in Equation [4] is very effective for linear problems, but requires multiple iterations for non-linear solutions to converge, since the stiffness must be iteratively reduced until either the solution converges (e.g., for $R < \text{FOS}$ in the SRM), or the problem is considered unstable because the solution does not converge (e.g., for $R > \text{FOS}$ in the SRM). See Figure 11 and note that the stiffness (slope of line) decreases significantly from the first to the second iteration.

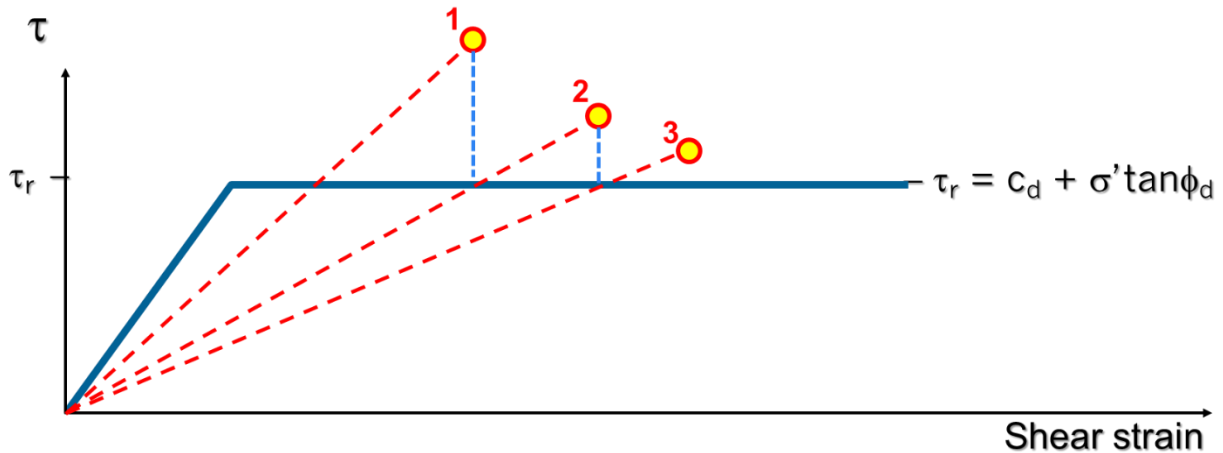


Figure 11 – First three iterations in the solution of a non-linear problem converging at large shear strains towards a shear stress $\tau = \tau_r$

Since the aim of the SRM is finding the threshold between stability and instability, the process described above is numerically very intensive for dense FE meshes around $R_{\max} = \text{FOS}$. To obtain R_{\max} (i.e. locate the threshold of instability) within reasonable computing times, FE programs often limit the number of iterations and/or use simplified convergence criteria based on energy, displacements and/or stiffness considerations. Unfortunately, these simplified criteria can result in numerical errors, especially when the stiffness matrix, $[SM]$, includes a combination of significantly different soil and structural stiffnesses.

Finite Difference solutions are obtained without the creation of a stiffness matrix; instead equations are solved, one grid element at a time, in an incremental and iterative procedure until equilibrium is satisfied. In FLAC, the equations of motions are used to solve all problems, regardless of their nature, and even static solutions are solved dynamically by incorporating a small amount of damping. Although solving problems dynamically makes FLAC inefficient for simple static problems, FLAC's use of a fast Lagrangian formulation largely compensates for the previously described inefficiencies; hence, the program is considered to run sufficiently fast for design purposes by practicing engineers. When $R > \text{FOS}$ in SRM analyses, the slope has insufficient strength which results in accelerations, velocities, and displacements within a portion of the mesh, instead of nonconvergence in a FE program; consequently, in SRM analyses FLAC's dynamic solution algorithm is considered an advantage as sudden accelerations in a slope model makes

landslide determination obvious and expeditious. Hence, for similar mesh densities, FLAC generally vastly outperforms FE programs in determining the threshold (R_{max}) between stability and instability, and it is generally considered the preferred computer program for SRM applications by practicing engineers.

2.8 Software Programs for SRM Analyses

2.8.1 FLAC/Slope

FLAC/Slope (Itasca, 2020b) is free-of-charge program that runs a limited set of instructions of the full FLAC program (Itasca, 2020a). Users can obtain SRM solutions for static problems with meshes of any size and unlimited number of materials, external loads, and anchorage systems. The program has the following limitations:

- Only static groundwater can be specified (i.e., seepage analyses cannot be performed).
- Strength criteria are limited to Mohr-Coulomb, Ubiquitous (with a single weak plane orientation), and Hoek-Brown.
- Only axial structural elements continuously bonded to the soil, such as soil nails, geogrids and geosynthetics, are allowed. Consequently, axial forces in tiebacks (which have an unbonded length) cannot be predicted; similarly, shear forces and bending moments cannot be predicted in grade beams, mat foundations, nor piles.
- FLAC/Slope uses identical and constant values of the initial elastic properties that cannot be changed. Since the aim of the SRM is to obtain the threshold between stability and instability, this approach is acceptable and computationally expeditious.

In the authors' opinion, the two main advantages of FLAC/Slope are its price (free) and its ease of use. Its main disadvantages include an automatic mesh generator that does not always work for complex cross-sections, and the lack of beam, pile and ground anchor (e.g., tieback) elements.

2.8.2 FLAC

The FLAC program (Itasca, 2020a) is a multi-purpose 2D finite difference program, that allows complex static and dynamic modeling, includes numerous advanced constitutive soil models and structural elements (including beams, piles and ground anchors), allows seepage and contaminant flow analyses, and includes thermal and dynamic computation capabilities.

It is the authors' opinion that the main disadvantage of FLAC is its complexity, which is in large part related to the enormous capabilities of the software, and it requires significant investment in training for new users. One of the main advantages of FLAC is its ability to run multiple scenarios in batch mode using a C-type computer language known as FISH (pronounced "Flacish"). The FISH language allows users to run the SRM in "manual mode" (i.e., manually reducing the strength until large displacements are predicted) and visualize the effects of the strength reduction factor,

R, as its value increases (as shown in Figure 3b). FISH can also be used for optimization purposes, as shown in Pradel, *et al.* (2010). Another advantage is FLAC's ability to interconnect structural elements, e.g., to connect the top of piles using grade beams in order to create a structural moment resisting frame, as shown in Figure 7b.

2.8.3 RS2

The RS2 program (Rocscience, 2019a) is a 2D finite element program for static analyses that includes a limited, but reasonable number of advanced constitutive soil models and structural elements, including soil nails, tiebacks, beams, and liners (liner elements are beam elements that develop shear stresses from their direct contact with the soil, such as mat foundations, grade beams, shotcrete walls, tunnel liners, etc.). RS2 finite element formulation allows both steady-state and transient seepage analyses.

In the authors' opinion, the main advantages of RS2 are its ease of use, and its ability to directly import LEM slope geometries from the SLIDE program (Rocscience, 2019b). RS2's main disadvantage is the lack of pile elements, although these may be modeled using wall elements when piles are closely spaced and provide full arching resistance.

2.8.4 Sigma/W

Sigma/W is a component of the GeoStudio software suite from GeoSlope International. It is a 2D finite element package that includes multiple constitutive soil models and structural elements (including beams and bars). GeoSlope recently (version 11.0, August 2020) added the strength reduction method of analysis as a built-in feature in Sigma/W.

In the authors' opinion, the main advantages of Sigma/W are its ease of use and the ability to perform LEM slope stability analyses and finite element analyses using the same geometry in a single model. The main disadvantage for SRM is the difficulty in determining the appropriate factor of safety from the results, as will be discussed below.

3 Design of Landslide Stabilization Piles Using LEM (GB 7)

The Ohio Department of Transportation designs drilled shafts for landslide stabilization according to Geotechnical Bulletin 7 (ODOT, 2020). The procedure is based on research performed by Dr. Robert Liang (Liang R. , 2002) and (Liang R. Y., 2010) who developed a software program called UA Slope. UA Slope performs slope stability analyses for a specified shear surface and includes the effects of soil arching between a single row of drilled shafts (piles). The percentage of the lateral load that is supported by the shafts is a function of the soil strength, the drilled shaft diameter, the center-to-center spacing of the drilled shafts, the horizontal location of the drilled shafts on the slope, and the slope of the ground surface. One will then take the results from

UA Slope and design the drilled shaft using the p-y method of analysis for laterally loaded piles. The general design procedure in GB 7 is as follows:

1. Perform a search for critical failure surface using limit equilibrium slope stability program of your choice.
2. Model the critical failure surface in UA Slope (the program does not include a search algorithm).
3. Try various drilled shaft geometries and anchor loads until desired safety factor is obtained.
4. Take the load on drilled shaft from UA Slope (and anchor load if applicable) and model the drilled shaft in LPile.
5. Design structural components of drilled shaft, and update LPile model.
6. Repeat LPile analysis until criteria for deflection, flexure and shear are satisfied.

The process is iterative and requires the use of three separate software programs. A LEM slope stability program such as Slope/W or SLIDE is required because UA Slope cannot search for the critical failure surface. The process does take into account the effect of soil arching between the drilled shafts. This is accounted for in the calculations performed by UA Slope.

For the case in which the slope below the stabilization piles will be left as-is and this slope has a safety factor equal to or greater than 1.30, GB 7 states that the actual passive resistance of the soil mass below the piles is reduced due to potential translation of the soil mass away from the piles. This is accomplished by reducing the group action p-multiplier in the LPile analysis by a factor equal to $(1 - 1/\text{FOS})$. For example, if the center-to-center spacing of the piles is equal to 3 diameters and $\text{FOS}=1.30$, then the group action p-multiplier is equal to 0.93 and the reduced p-multiplier above the shear surface is equal to $0.93 (1 - 1/1.30) = 0.215$.

For the case in which the slope below the stabilization piles will be left as-is and this slope has a safety factor less than 1.30, GB 7 states that the slope below the piles should be considered unstable and the analysis must consider the anticipated loss of passive resistance from the soil downslope of the piles. This is done in the LPile analysis by lowering the ground surface, thus discounting the passive resistance between the actual ground surface and the artificially lowered ground surface in the analysis. The ground surface is lowered by the amount calculated by the formula below.

$$d_t \tan \beta_{dh} \quad [5]$$

where:

$$\begin{aligned} d_t &= \text{depth to the shear surface at the location of the piles} \\ \beta_{dh} &= \text{angle of slope from horizontal} \end{aligned}$$

For slopes where $\beta_{dh} = 45$ degrees or steeper, the entire soil mass above the shear surface is neglected.

4 Comparison of Analyses Results

4.1 Slope without Stabilization Piles, OTT-2-27.18

The OTT-2-27.18 project was an embankment failure that occurred in 2017 near Sandusky, Ohio. The stabilization repair consisted of excavating the failed embankment and constructing a toe key filled with dump rock at the base of the embankment, and then rebuilding the embankment. The original LEM stability analysis was performed by Stantec using Slope/W. Stantec provided their input file for our use in this study. The first set of LEM stability analyses were performed using the Morgenstern-Price analysis method, which is the default analysis method in Slope/W. Our results matched Stantec, as would be expected, and we then ran the analysis using the Bishop and Spencer analysis methods. Five different models were analyzed, consisting of the existing post-failure conditions (with and without a zone of residual strength soil), an undrained analysis during construction, and two long-term drained analyses for the final configuration, one with the failure surface going through the toe key and one with the failure surface above the toe key. The analyses were then repeated in SLIDE. The results are shown in Table 1. The factors of safety were generally the same or very close between the two programs, with the largest difference occurring in the long-term drained analysis with the failure surface above the toe key (1.29 vs 1.37). The safety factors calculated using the Bishop method were lower than the safety factors calculated using the more rigorous Spencer and Morgenstern-Price methods, however this is not surprising as the Bishop method was originally developed for circular surfaces and its equations are based on moment equilibrium for the entire surface of failure with respect to a center of rotation; hence, for noncircular surfaces the Bishop method ignores the effect of shear forces between slices which can have a significant effect on sections such as in the OTT-2 project where the critical failure is controlled by a long horizontal weak layer (Figure 12). Therefore, the safety factors from the Spencer and Morgenstern-Price method are preferred for comparison to the SRM safety factors.

Table 1 – Safety Factor for Slope at OTT-2-27.18

OTT-2	LEM ¹			SRM		
		Slope/W	SLIDE	RS2	FLAC/Slope	Sigma/W
Existing w/o Residual	Bishop	0.98	0.93	0.98	0.99	1.05 – 1.25
	Spencer	1.00	1.01			
	M-P	1.00	1.00			
Existing with Residual	Bishop	0.90	0.85	0.91	0.92	-- ²
	Spencer	0.92	0.92			
	M-P	0.92	0.92			
Digout Undrained	Bishop	1.12	1.10	1.17	1.20	-- ²
	Spencer	1.16	1.16			
	M-P	1.15	1.15			
Digout Drained (through key)	Bishop	1.19	1.12	1.23	1.21	1.0 – 1.5
	Spencer	1.29	1.26			
	M-P	1.29	1.27			
Digout Drained (above key)	Bishop	1.26	1.25	1.23	1.21	1.0 – 1.5
	Spencer	1.29	1.37			
	M-P	1.30	1.37			

¹ : Lowest LEM numbers from Spencer and M-P are bold for each analysis

² : Not reported due to convergence difficulties

We then performed the SRM analyses in RS2 and Sigma/W, and we then recreated the model in FLAC/Slope. Four different models were run, two for the existing conditions, one for the undrained condition during construction, and one for the long-term drained condition. Because one does not specify limits on the potential failure surface in the SRM analysis, the results from the two LEM analyses for the long-term drained condition are compared to one result from the SRM. The results from RS2 and FLAC/Slope were close to the safety factors from the LEM analysis using either the Spencer or Morgenstern-Price methods for the existing conditions and the undrained construction case. For the long-term drained condition, the RS2 and FLAC/Slope safety factors were approximately 0.03 to 0.05 lower than the comparable lowest LEM safety factors. Figure 12 shows the results from FLAC/Slope and RS2 for the long-term drained condition.

When we attempted to perform SRM analysis of the OTT-2 project using Sigma/W, we encountered difficulties determining an appropriate strength reduction factor that would indicate failure of the slope. Typically, the appropriate strength reduction factor for failure is indicated by one or more of the following conditions in a FE analysis: failure of the model to converge, very large displacements, increased unbalanced energy, or sharply decreased stiffness of the domain. In our models for OTT-2 we did not observe any of these conditions within the range of expected strength reduction factors. All models converged, and displacements gradually increased without a sharp increase at any particular value of R (Figure 13). Unbalanced energy either increased or remained steady, and domain stiffness either decreased gradually or even increased (Figure 14 and Figure 15). As a result, we were not able to determine the safety factor using Sigma/W. The SRM

is a recent addition to the Sigma/W program and we have not used its SRM feature before this study. Consequently, the author (Narsavage) who had access to Sigma/W consulted GeoSlope support with the issue. As a result of that communication, GeoSlope has made changes to the software code and will release an update to the software that will include improvements that address the issue. They shared graphs of unbalanced energy and domain stiffness that show distinct changes at appropriate strength reduction factors after the code revisions. Unfortunately, the update had not been released before publication of this report.

As explained in Section 2.7, convergence assessments are important for FE methods due to the iterative nature of the solution in Equation [4]. Plots in Figure 16 to Figure 19 show the predicted maximum total displacements as a function of the Strength Reduction Factor, R , using RS2 (the other FE program used in this study), and indicated whether convergence was achieved or not after the maximum number of iterations was reached (default=500). Convergence plots are not provided by FLAC/Slope, nor are they considered relevant. Users can get equilibrium ratio and unbalanced force plots in FLAC but for $R > FOS$ these plots are not comparable to those from RS2 or Sigma/W since the dynamic solution in FLAC results in accelerations, velocities and displacements that are not predicted by these FE programs.

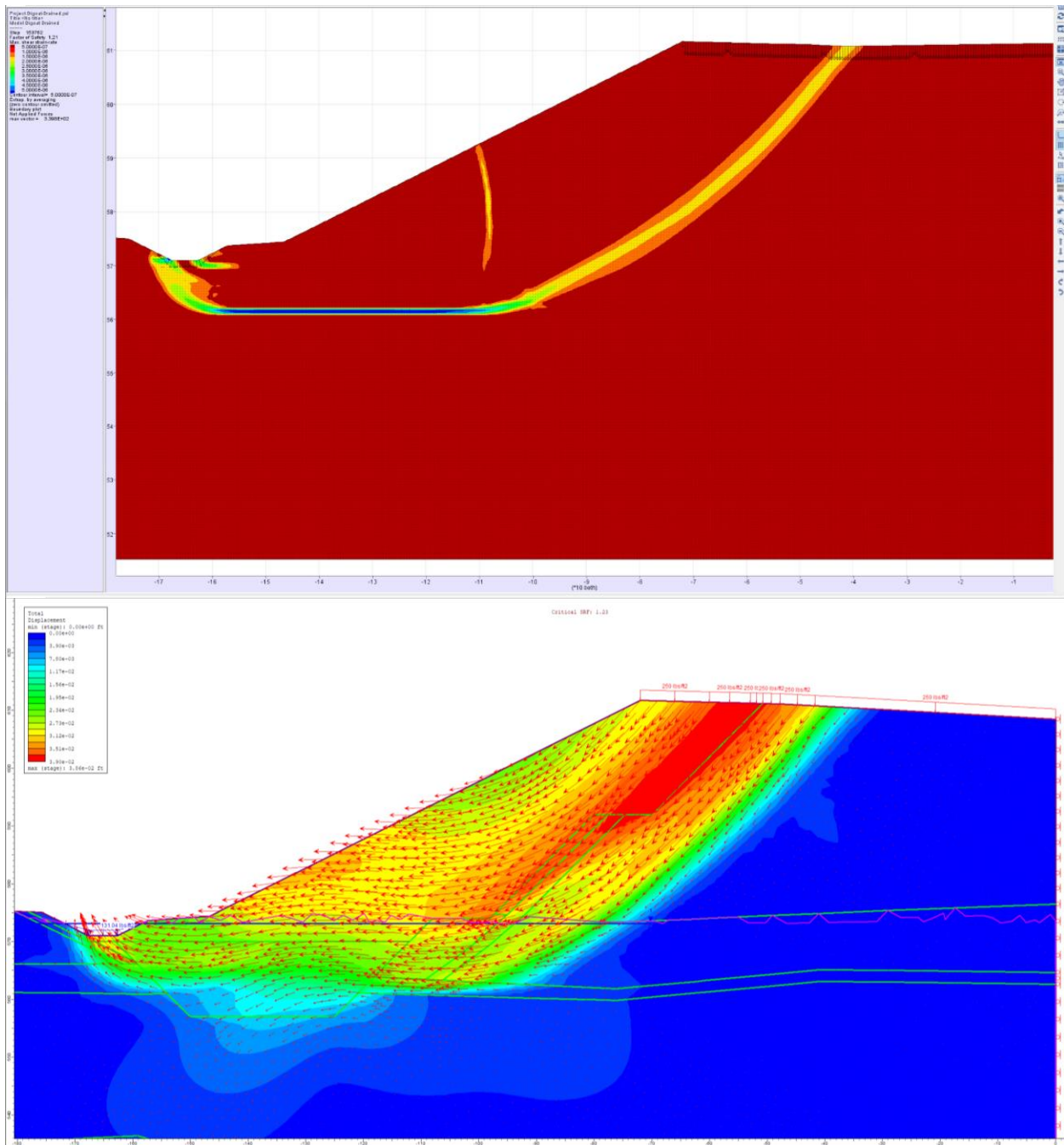


Figure 12 – OTT-2 Digout Drained Conditions, Shear Strain from FLAC/Slope (top) and total displacements from RS2 (bottom)

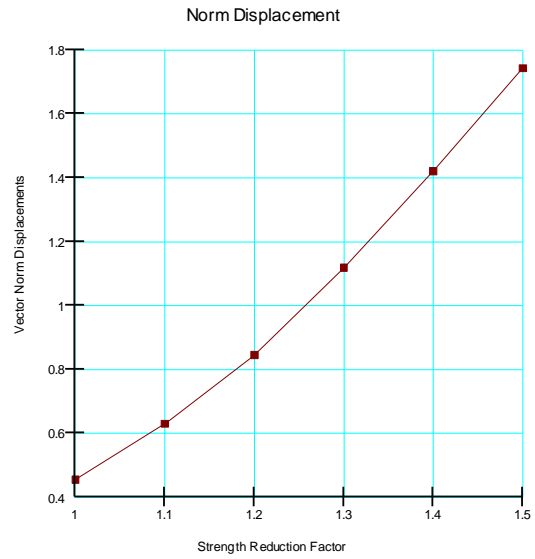
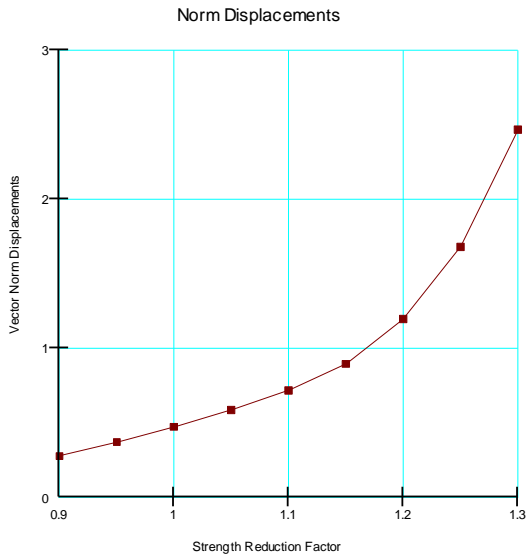


Figure 13 – Vector Norm Displacements for OTT-2 from Sigma/W
Left - ex. conditions, w/o residual; Right digout, drained conditions

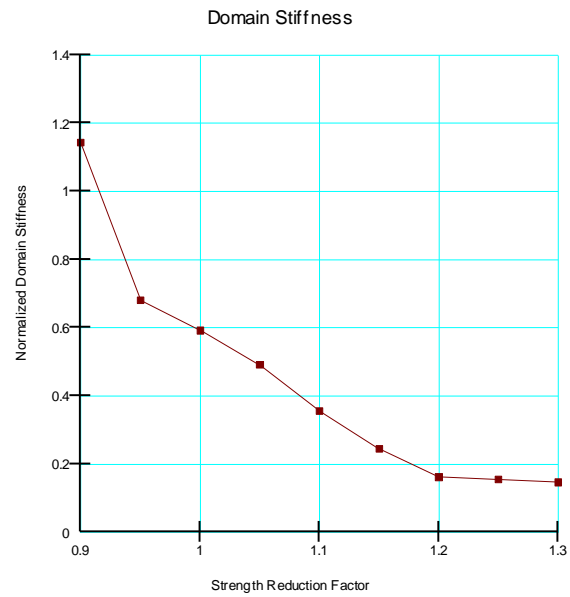
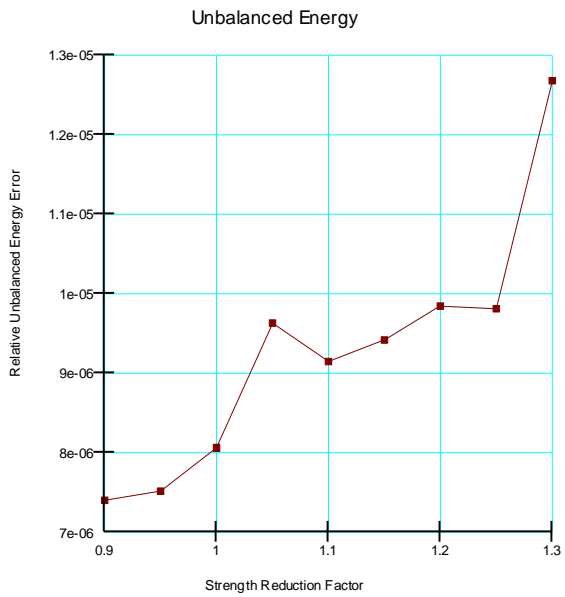


Figure 14 – Unbalanced Energy and Domain Stiffness
for OTT-2 ex. conditions, w/o residual from Sigma/W

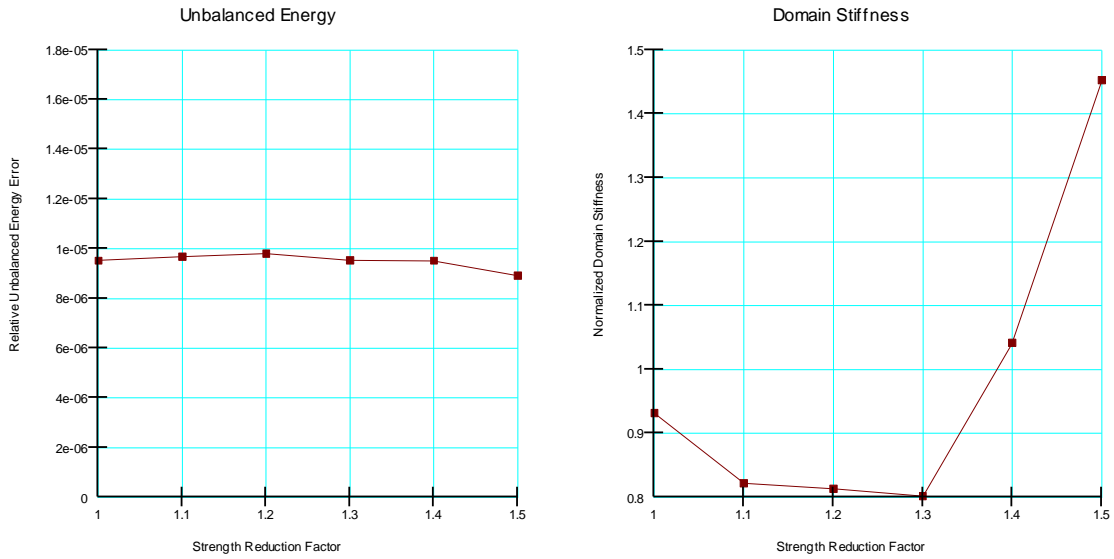


Figure 15 – Unbalanced Energy and Domain Stiffness for OTT-2 digout, drained conditions from Sigma/W

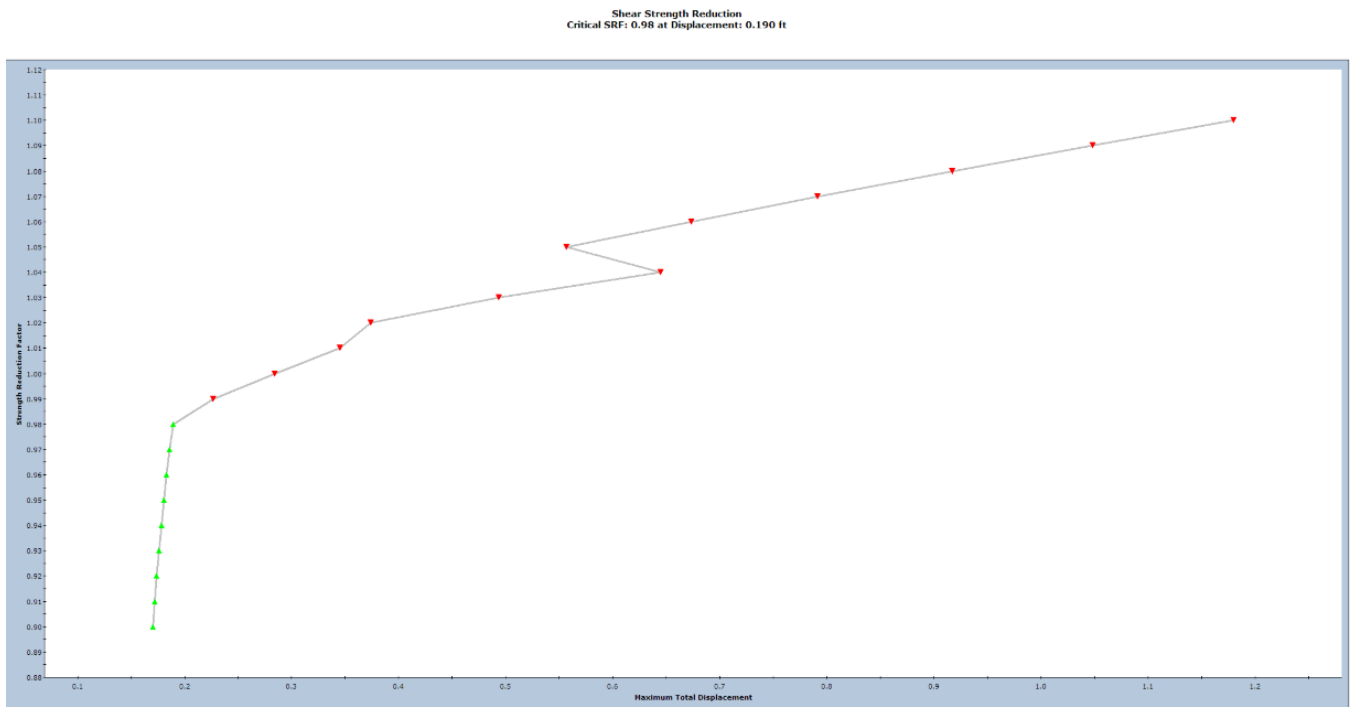


Figure 16 – SRM Convergence Plots for OTT-2 ex. conditions, w/o residual from RS2

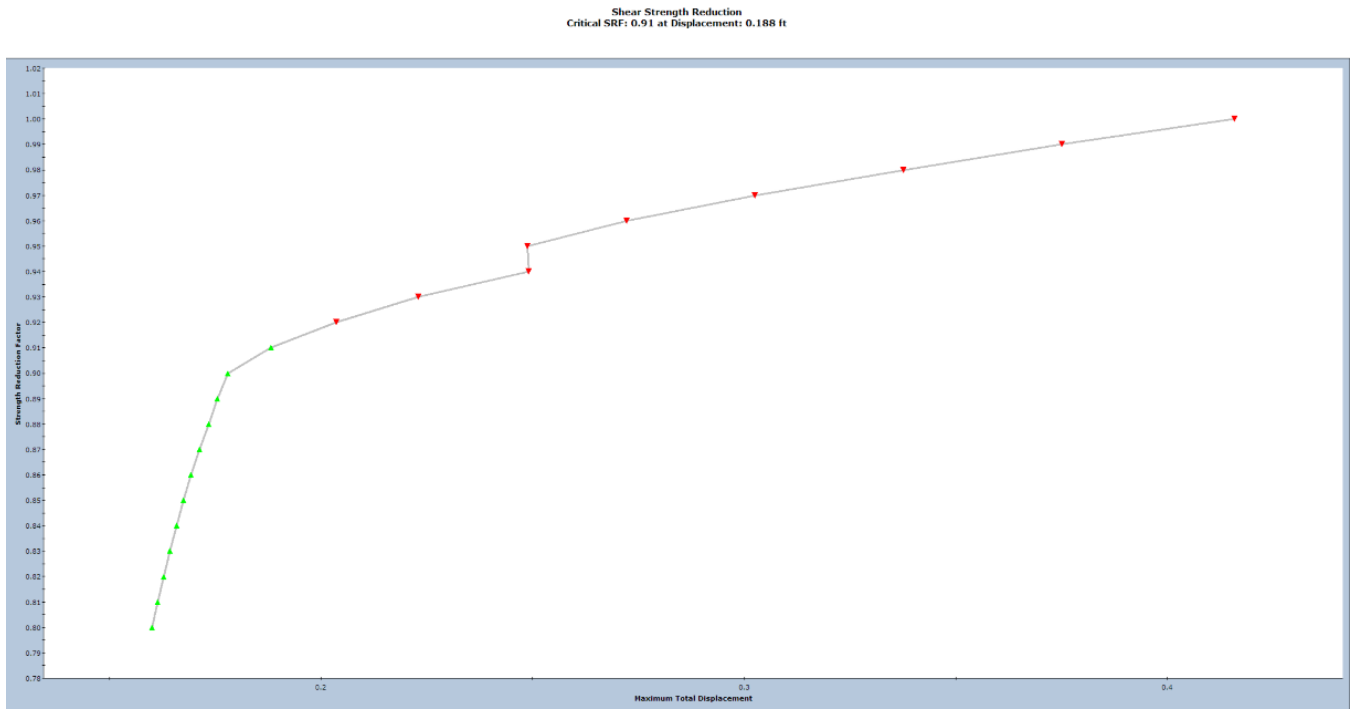


Figure 17 – SRM Convergence Plots for OTT-2 ex. conditions, with residual from RS2

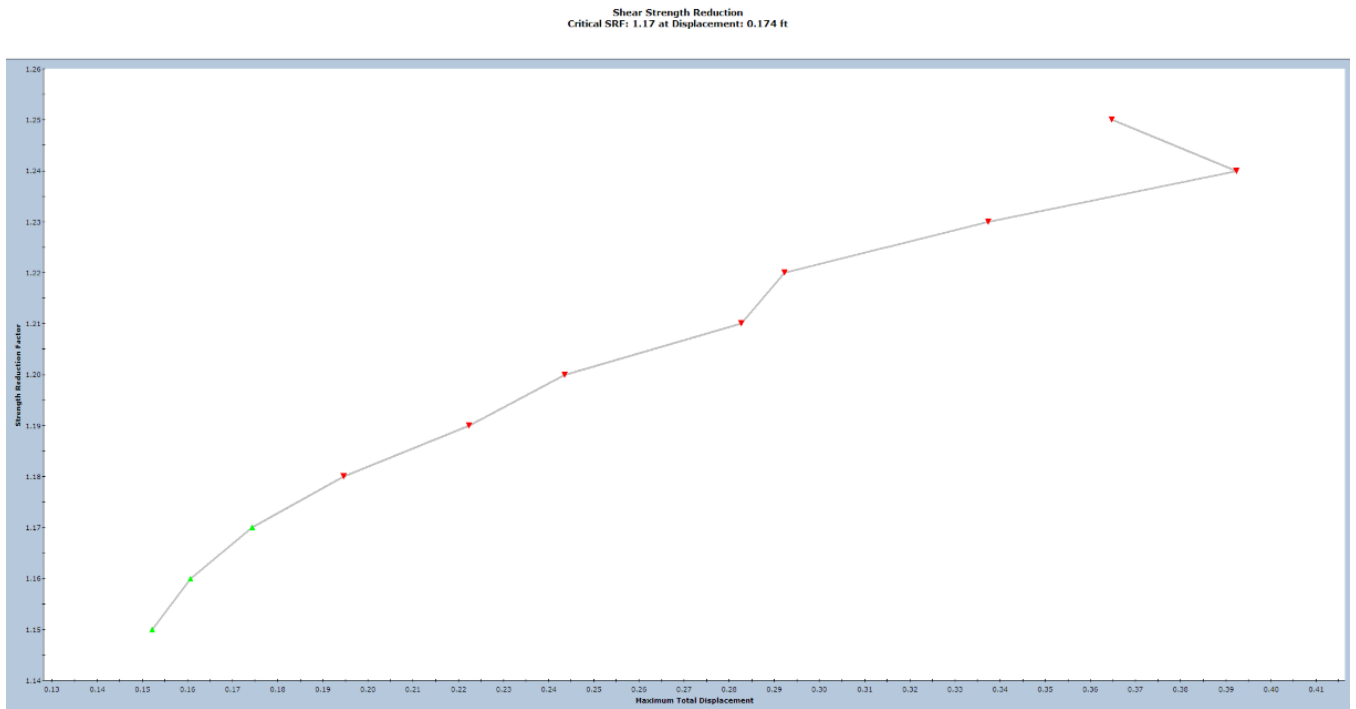


Figure 18 – SRM Convergence Plots for OTT-2 digout undrained conditions from RS2

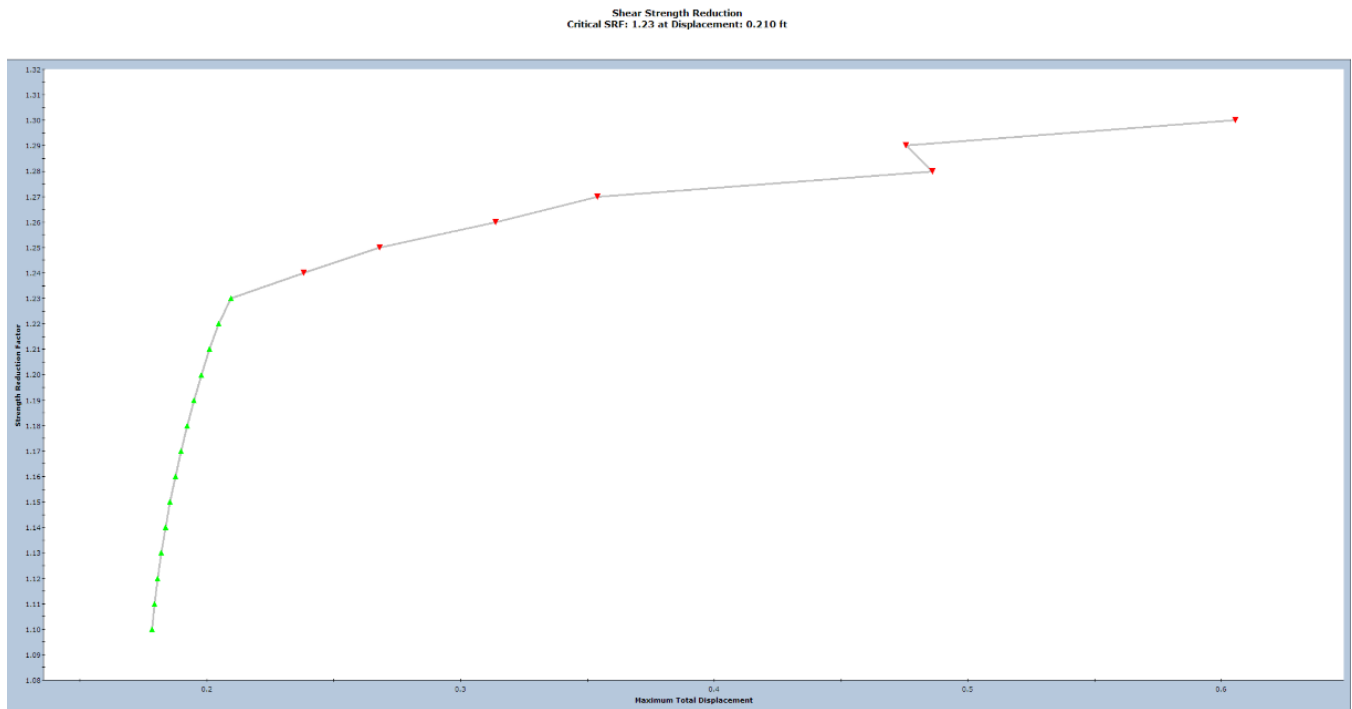


Figure 19 – SRM Convergence Plots for OTT-2 digout drained conditions from RS2

4.2 Slope with Stabilization Piles, MUS-16-6.70

The MUS-16-6.70 project is a slope failure along SR 16 in Muskingum County, Ohio, approximately 15 miles north of Zanesville. The site exploration and landslide investigation were performed by the ODOT Office of Geotechnical Engineering in 2020. ODOT provided the soil profile and relevant soil parameters for the analyses. Based on right-of-way limitations, the landslide stabilization method is anticipated to be a single row of drilled shafts or retaining wall. For the purposes of this study, we analyzed a single row of drilled shafts. Due to the resulting loads on the drilled shafts, we included a rock anchor at the top of the drilled shaft to provide additional support. Using the procedures described in GB 7, we designed the following stabilization structure.

- 4-foot diameter drilled shafts, spaced 8 ft apart (located at x=120 ft in the cross-section)
- 80 ft long, reinforced concrete with rebar cage and steel W-section core.
- 12 - #10 reinforcing bars (with 3-inch cover)
- W40x149 steel section in center
- 4-strand rock anchor, inclined 25 degrees from horizontal, 125 kip lock-off load

These structural elements were then modeled in the SRM analyses. The resulting safety factors are presented in Table 2. The bending moment in the pile and the load in the anchor are presented in Table 3.

Table 2 – Safety Factor for Slope at MUS-16-6.70

MUS-16	LEM ¹			SRM			
		Slope/W	SLIDE	UA Slope	RS2	FLAC	Sigma/W
Existing Conditions	Bishop	0.99	0.95	0.99	0.96	0.95	1.0-1.15
	Spencer	1.00	1.00				
	M-P	1.00	0.99				
Ex. Shear Surface With Pile and Anchor		--	--	1.32	--	--	--
Slope Below Pile	Bishop	1.14	1.10	--	1.13	1.13	1.05-1.3
	Spencer	1.15	1.17				
	M-P	1.15	1.17				

¹ : Lowest LEM numbers from Spencer and M-P are bold for each analysis

Table 3 – Stabilization Pile Results

MUS-16	GB 7	FLAC	RS2 ¹	Sigma/W
ΔFOS: Increase in FOS	0.33	0.18	0.17	N/A
M _{max} : Maximum Bending Moment in Piles (lbs.ft)	3.98E+06	2.10E+06	2.03E+06	8.64E+04 (R=1.15) 1.14E+05 (R=1.30)
M _{max} / ΔFOS (lbs.ft)	1.21E+07	1.17E+07	1.19E+07	N/A
Maximum Anchor load (lbs) Prestress = 1.25E+05	1.25E+05	1.31E+05	1.25E+05	1.41E+05

¹ : Piles modeled using continuous beam elements since RS2 does not have pile elements

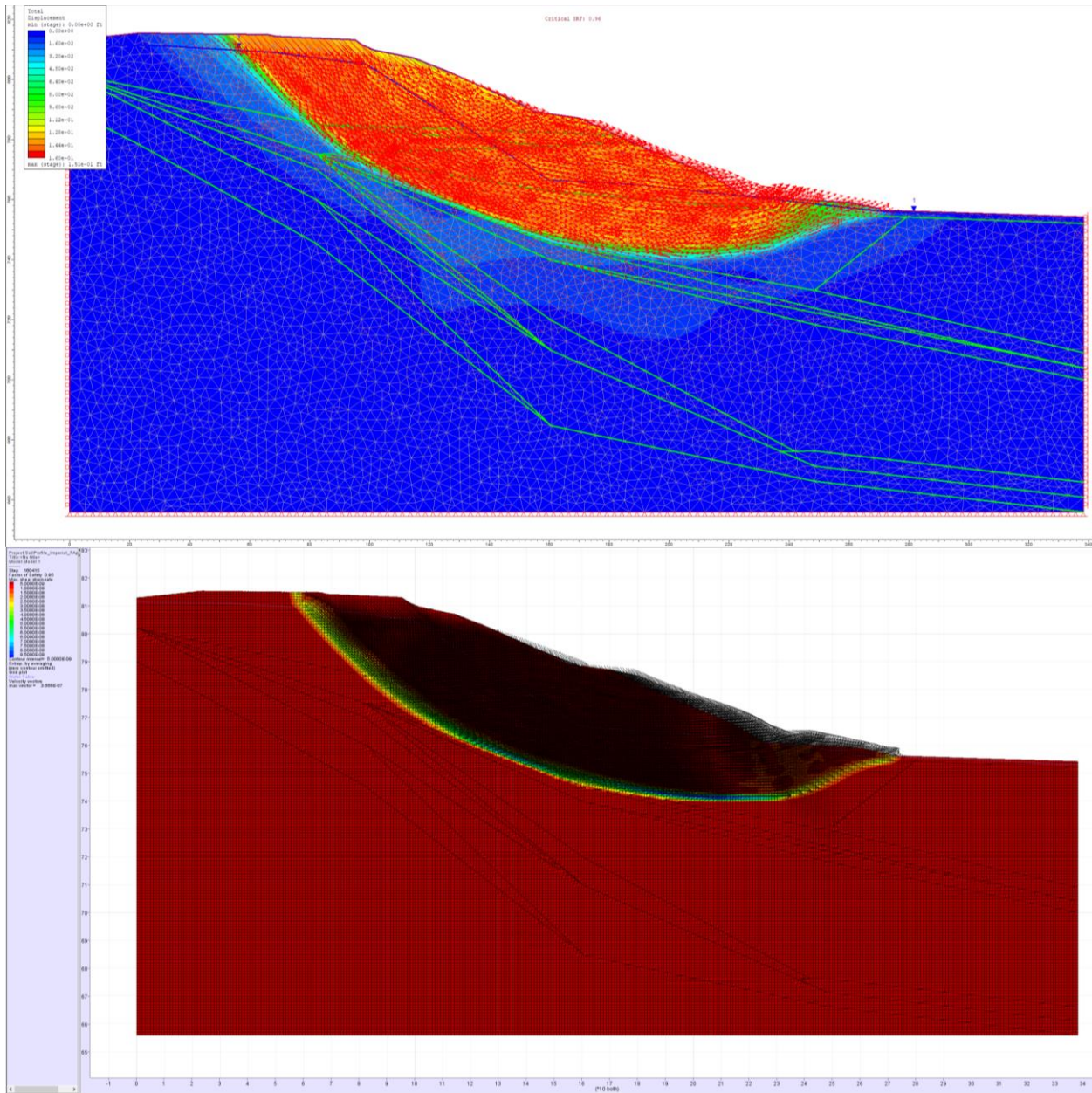


Figure 20 – MUS-16 Existing Conditions, Displacements from RS2 (top) and FLAC/Slope (bottom)

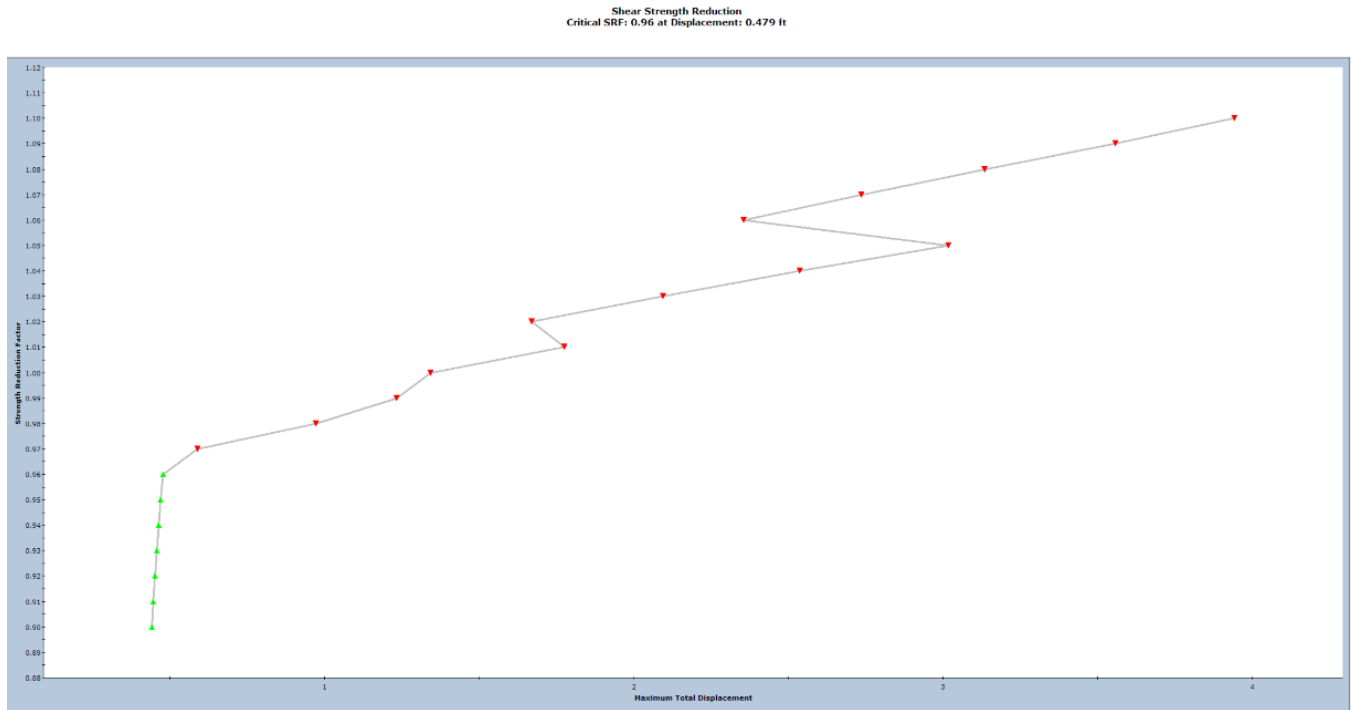


Figure 21 – MUS-16 Convergence Plot from RS2

The slope stability LEM analyses of the existing conditions were performed using the Bishop, Spencer, and Morgenstern-Price methods, using Slope/W and SLIDE. The critical failure surfaces were similar in shape and encompassed the entire slope. The location of the scarp in the critical failure surface was about 10 to 20 feet behind the observed scarp location. The factors of safety were generally the same or very close between the two programs, having values of 0.99 or 1.0 except for the Bishop method in SLIDE, which had a result of 0.95. The critical failure surface from Slope/W was also analyzed using UA Slope and resulted in a safety factor of 0.99. The safety factors from FLAC and RS2 were slightly lower at 0.95 and 0.96. As before with the OTT-2 project, we found it difficult to determine the appropriate safety factor using Sigma/W. The graphs for unbalanced energy, domain stiffness, and vector norm displacements from Sigma/W are shown in the Figure 22. Only the vector norm displacement graph indicates a change between strength reduction factors of 1.15 to 1.30. The graphs for unbalanced energy and domain stiffness do not show a clear break at an appropriate strength reduction factor.

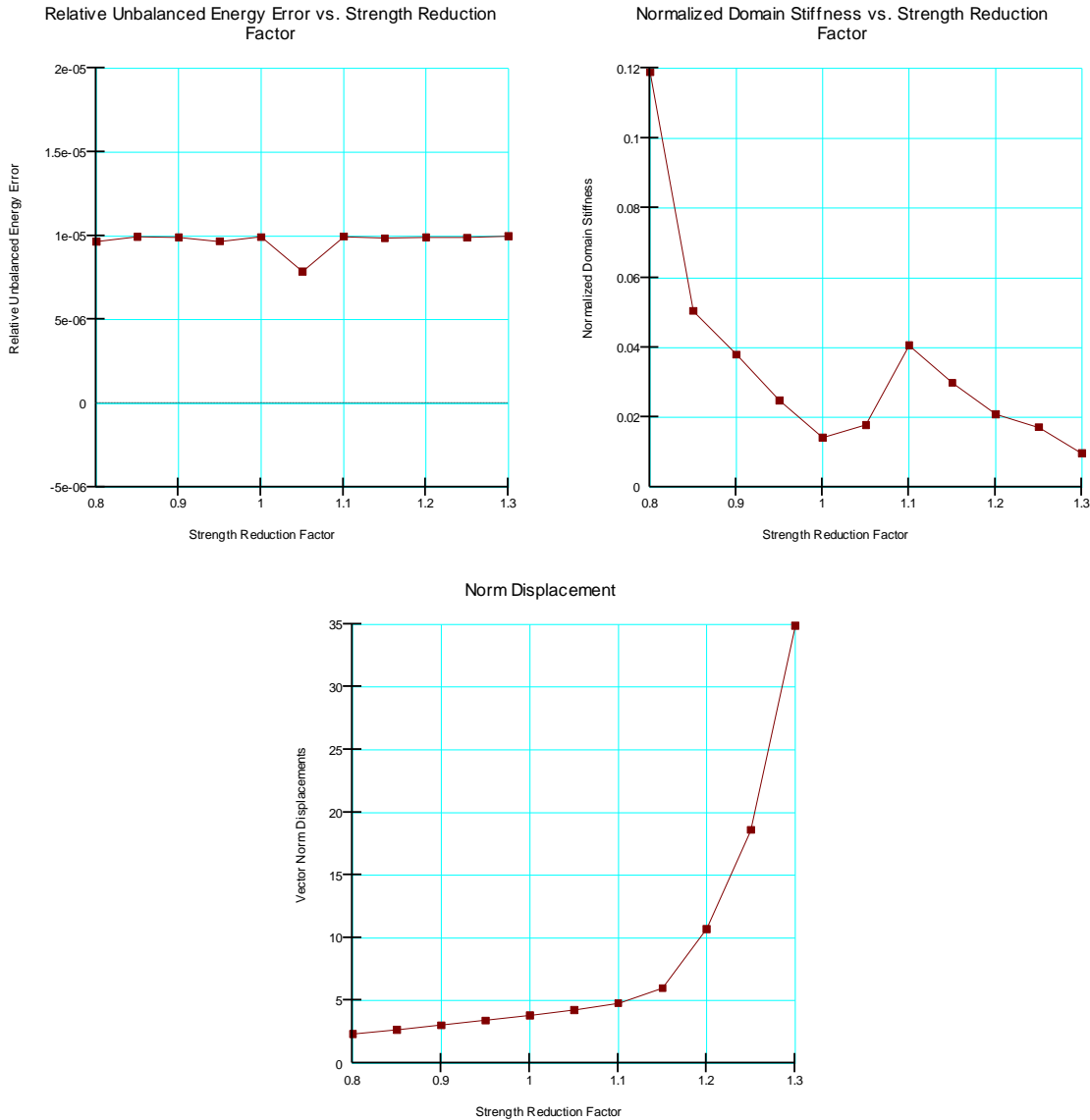


Figure 22 – Unbalanced energy, Domain Stiffness, and Vector Norm Displacement for MUS-16 for ex. conditions from Sigma/W

Using the methods described in GB 7, we used UA Slope to determine the stabilization pile location, spacing and diameter. We then took the resulting load on the pile from UA Slope and analyzed the pile using LPile to determine the moment in the pile. After an initial analysis, we decided a rock anchor at the top of the pile was required, and we revised the analysis to include the rock anchor. Once we determined the structural properties of the pile, we included the pile in the SRM analysis models. It was at this point that we encountered a limitation of the SRM. The factor of safety for the slope below the pile was about 1.13. Consequently, the SRM analysis was not able to give meaningful results for strength reduction factors greater than 1.13. We confirmed the safety factor of the slope below the piles with Slope/W and SLIDE, which provided slightly larger safety factors of 1.15 and 1.17 for Spencer and Morgenstern-Price, and 1.14 to 1.10 for the

Bishop method. As before, we were not able to determine the appropriate safety factor using Σ/W .

The maximum bending moment in the pile for each analysis method is shown in Table 3. Note that pile moments from SRM are limited by $FOS=1.13$, i.e., the Factor of Safety of the slope below the piles (Figures 3 and 4). Figure 23 shows the predicted maximum bending moment based on displacements using FLAC up to the point when the slope becomes unstable.

Because LEM analyses for failure planes through the piles ignore more critical mechanisms (e.g., failure below the piles) pile bending moments based on a safety factor of 1.32 could be calculated using GB 7. In one of the author's opinion (Pradel), designing piles for loads corresponding to $FOS = 1.32$ when the slope has a $FOS = 1.13$ should be carefully considered. Nevertheless, note that when the relative gain in FOS is considered, e.g., by normalizing the increase in bending moments using the ratio $M_{max} / \Delta FOS$, the results obtained by GB 7, FLAC and RS2 are quite similar.

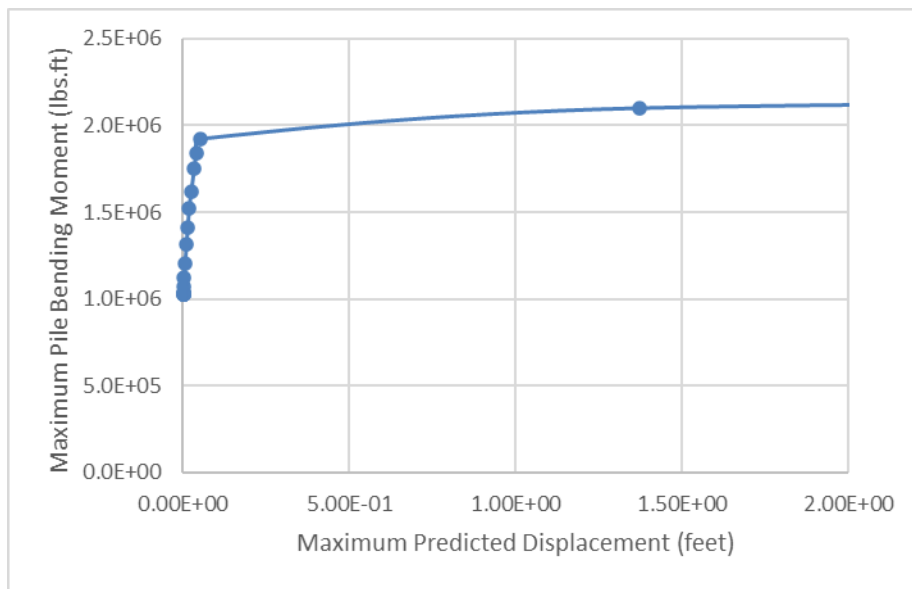


Figure 23 – Determination of Reasonable Maximum Bending Moment for MUS-16 using FLAC.

The rock anchor was designed with a prestress load of 125 kips and was modeled as such in the SRM models. FLAC indicated the anchor load increased slightly to 131 kips due to displacements. RS2 did not indicate any increase in the anchor load, and it is not possible to predict the potential anchor load change using the methods of GB 7.

5 Recommendations for SRM

5.1 When to use SRM

When one is analyzing a stabilization structure that consists of more than one row of piles, the SRM must be used, as the methods described in GB 7 cannot accommodate more than one row of piles. In this case we recommend analyzing the existing, unstable slope with both SRM and LEM to check if the results are similar. If they are not, then one should examine the models for both methods and check for discrepancies, as the two methods should give similar results for unreinforced slopes. After this has been done, then one can add the stabilization structure to the model and perform the SRM analysis for the new conditions.

If the stabilization structure consists of a single row of piles, then either SRM or the methods described in GB 7 may be used to analyze the stabilized slope. The choice in this case should be based on the engineer's experience and familiarity with the different analysis methods. However, when the installation of stabilization piles results in the minimum critical failure surface being above or below the row of piles, such as the MUS-16 project, then both the LEM and SRM have limitations. SRM analyses are limited by the minimum safety factor of the entire slope. For example, on the MUS-16 project the SRM could only give results for a safety factor of 1.13, as this was the minimum safety factor for the slope below the piles. Demands beyond the factor of safety of the entire slope (FOS) may be normalized (as shown in Table 3) and the normalized gain used to estimate demands beyond FOS; however, the practice of designing piles on a slope (e.g. MUS-16, for $FOS = 1.32$) when the slope has only a $FOS = 1.13$ appears uneconomical and should be carefully considered. The LEM can predict the loading on the piles for a safety factor of 1.32, but this may not be realistic as the soils on the downslope side of the piles would not provide full passive resistance at this safety factor level. In an attempt to address this issue GB 7 reduces the soil support below the pile within the LPILE analyses.

When the slope stabilization does not include reinforcing piles, such as excavating the embankment and constructing a toe key as in the OTT-2 project, both LEM and SRM should provide similar results, although the SRM may require more effort for some users to prepare the model and more time to perform the analyses. However, when subsurface conditions are complex, it is beneficial to use the SRM to ensure the LEM search parameters have not caused the search algorithm to miss the critical non-circular failure surface. If the SRM does identify a more critical failure surface, then the search parameters can be adjusted in the LEM to analyze similar failure surfaces and compare the resulting safety factors.

5.2 Soil Model and Soil Properties

The Mohr-Coulomb failure criterion is generally used to obtain FOS by the SRM. As shown in Figure 1, in addition to the cohesion, c , and friction angle, ϕ , implementation of the SRM in

numerical programs also require elastic properties (e.g., the elastic modulus, E , and the Poisson's ratio, ν) in order to obtain predictions at small strains. Since the aim of the SRM is to find the threshold between stability and instability, predictions for reduction factor around R_{\max} generate large strains and displacements. Therefore, SRM predictions are generally not sensitive to values of elastic parameters. Recognizing that elastic properties are only important at small strains, certain numerical programs use default values that the user cannot change (e.g., in FLAC/Slope, a bulk modulus $K = 1E+08$ psf and a shear modulus $G = 3E+07$ psf are used). The default values from FLAC/Slope may be used across materials in other programs (e.g., RS2) when no stiffness information is available, or can be obtained through measurements or correlations (e.g., from shear wave velocity measurements or CPT correlations). Alternatively, typical values, as given by AASHTO or FHWA may be used.

For rock deposits, the non-linear Hoek-Brown criteria is a common alternative to the Mohr-Coulomb failure criterion in most SRM programs; note that SRM programs also allow weak planes to be specified within a rock mass at a specified angle (e.g., to model fractures, bedding, planes of weakness, etc.).

5.3 Soil-Structure Interaction (spring models used to connect soil and pile meshes)

For landslide stabilizing piles, we recommend that springs be modeled for simplicity as bi-linear springs (as depicted in Figure 9) in all relevant directions, i.e., for skin friction, end bearing and perpendicular to the shaft (p-y). The maximum lateral resistance of the springs may be modelled in the following manner:

For center-to-center spacings $S < 3D$:

- Formulation for pile elements (preferred method, e.g., using FLAC): full arching may be assumed with $p_{\max} = S \cdot K_p \cdot \sigma_z$ to obtain the maximum lateral load a pile exerts on the subsurface.
- Formulation for beam elements (acceptable but not the preferred method, e.g., using RS2): since full arching may be assumed between closely spaced piles, and the piles act as a continuous retaining wall, beam elements may be used for modeling purposes.

For center-to-center spacings $S > 3D$:

- Beam elements are not appropriate since they do not allow soil to flow between piles. Hence, a program having pile elements must be used (e.g., FLAC).
- Springs' lateral resistance (p_{\max}) may be obtained from either material-appropriate p-y curves, or preferably, pushover analyses performed at multiple depths for the different materials (e.g., Figure 10).

The 3D threshold for spacing is based conservatively on arching principles on the research by Broms described in Section 2.6, above. The initial stiffness of the springs (e.g., $k_{p-y}=p_{max}/d_{ref}$) can be obtained from the p_{max} recommended above and a material appropriate displacement d_{ref} (typical values of d_{ref} are shown for the p-y springs in Figure 9).

5.4 General Recommendations for SRM

- In order to reduce the computation time at the beginning of the analysis, one should start with a wide bracket of strength reduction factors and a large increment. For example, set the initial $R=0.5$, the final $R=2.0$, and the increment at 0.25, for a total of seven runs. After the initial results, one can refine the bracket and reduce the increment size.
- **Remote Failures:** Occasionally a mesh may exhibit slope failures in a remote location from the area being investigated (e.g., Figure 24). Such areas should be excluded from consideration (e.g., by locally increasing the soil strength) as the SRM cannot provide meaningful results for $R > FOS$;

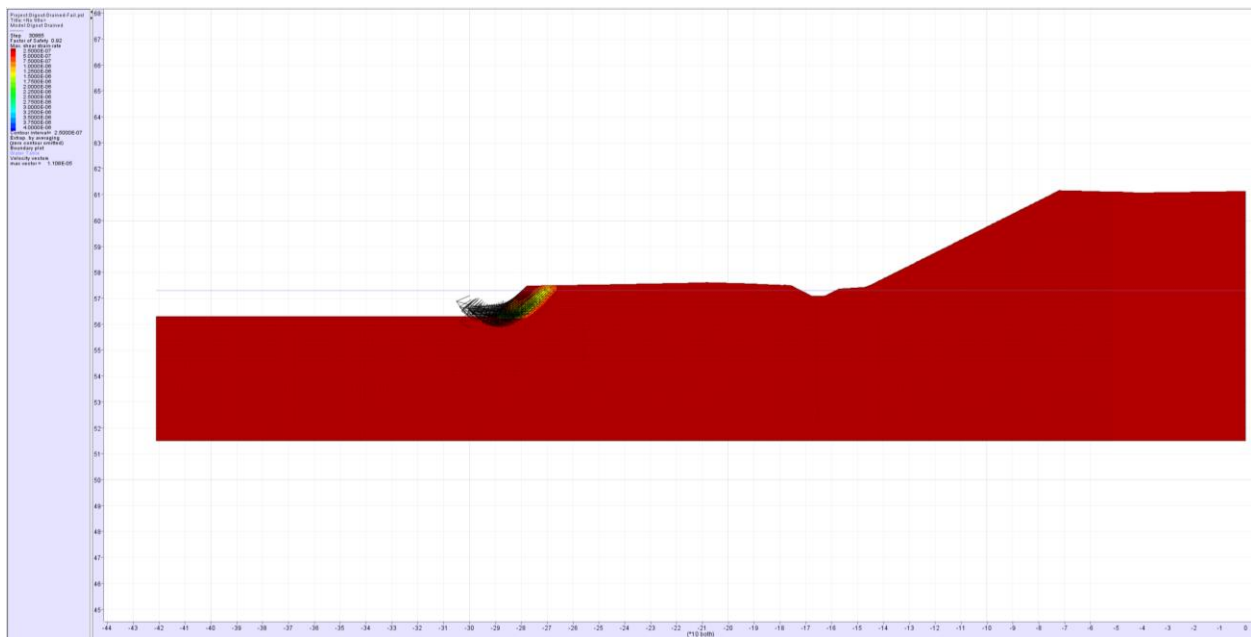


Figure 24 – Local slope instability in an area away from the slope being stabilized

- **FOS < 1 cross-sections:** Occasionally a slope model may have a FOS less than one for its initial conditions. In FE and FD programs, piles must be installed in stable ground. One should increase the stability of the model by temporarily lowering the water level in the model or by appropriately increasing the soil strength in the step where the piles are introduced. The water level or soil strength can be returned to the adopted initial conditions in subsequent computation steps.

6 References

- Bentley. (2019). PLAXIS 2D Finite Element Program Version 20. Delft, Netherlands. Retrieved from www.plaxis.com
- Broms, B. B. (1964a). Lateral resistance of piles in cohesionless soils. *Journal of the soil mechanics and foundations division*, *90*, 123–156.
- Broms, B. B. (1964b). Lateral resistance of piles in cohesive soils. *Journal of the soil mechanics and foundations division*, *90*, 27–63.
- Carder, D. R., & Temporal, J. (2000). A review of the use of spaced piles to stabilise embankment and cutting slopes. *TRL REPORT 466*.
- Duncan, J. M. (1996). State of the art: limit equilibrium and finite-element analysis of slopes. *Journal of Geotechnical engineering*, *122*, 577–596.
- Duncan, J. M., & Wright, S. G. (2005). *Soil strength and slope stability*. John Wiley & Sons.
- Ensoft. (2019). Computer Program LPILE Version 11. Austin, Texas, USA. Retrieved from www.ensoft.inc
- Griffiths, D. V., & Lane, P. A. (1999). Slope stability analysis by finite elements. *Geotechnique*, *49*, 387–403.
- Hassiotis, S., Chameau, J. L., & Gunaratne, M. (1997). Design method for stabilization of slopes with piles. *Journal of Geotechnical and Geoenvironmental Engineering*, *123*, 314–323.
- Itasca. (2020a). FLAC (Fast Lagrangian Analysis of Continua) Version 8.1. Minneapolis, Minnesota, USA. Retrieved from www.itasgacg.com
- Itasca. (2020b). FLAC/Slope Slope Stability Program Version 8.1. Minneapolis, Minnesota, USA. Retrieved from www.itascacg.com
- Ito, T., & Matsui, T. (1975). Methods to estimate lateral force acting on stabilizing piles. *Soils and foundations*, *15*, 43–59.
- Ito, T., Matsui, T., & Hong, W. P. (1981). Design method for stabilizing piles against landslide—one row of piles. *Soils and Foundations*, *21*(1), 21–37.
- Liang, R. (2002). *Drilled shaft foundations for noise barrier walls and slope stabilization*. University of Akron. Dept. of Civil Engineering.
- Liang, R. Y. (2010). *Field instrumentation, monitoring of drilled shafts for landslide stabilization and development of pertinent design method*. Columbus, OH: Ohio. Dept. of Transportation, FHWA/OH-2010/15.
- Liang, R., & Zeng, S. (2002). Numerical study of soil arching mechanism in drilled shafts for slope stabilization. *Soils and foundations*, *42*, 83–92.

- LimitState. (2017). LimitState:Geo computer program. Sheffield, UK. Retrieved from www.limitstate.com
- NAVFAC. (1986). 7.01: Soil Mechanics Design Manual. *Department of the Navy, Naval Facilities Engineering Command, Alexandria, VA, USA.*
- Newmark, N. M. (1965). Effects of earthquakes on dams and embankments. *Geotechnique*, 15(2), 139–160.
- ODOT. (2020). Geotechnical Bulletin 7: Drilled shaft landslide stabilization design. Columbus, Ohio, USA: Ohio Department of Transportation. Retrieved from www.dot.state.oh.us/Divisions/Engineering/Geotechnical/Geotechnical_Documents/GB7_Drilled_Shafts.pdf
- Poulos, H. G. (1995). Design of reinforcing piles to increase slope stability. *Canadian Geotechnical Journal*, 32(5), 808-818.
- Pradel, D. (2018). Case History: The Estrondo Landslide Stabilization in Encino, California. In *IFCEE 2018* (pp. 232–244). doi:10.1061/9780784481622.019
- Pradel, D., Garner, J., & Kwok, A. O. (2010). Design of Drilled Shafts to Enhance Slope Stability. In *Earth Retention Conference 3* (pp. 920–927). doi:10.1061/41128(384)92
- Prakash, S., & Saran, D. (1967). Behavior of laterally-loaded piles in cohesive soil. *Asian Conf Soil Mech & Fdn E Proc/Is/*.
- Rocscience. (2019a). RS2-2019 Finite Element Program. Toronto, Canada. Retrieved from www.roscience.com
- Rocscience. (2019b). SLIDE-2019 Slope Stability Program. Toronto, Canada. Retrieved from www.roscience.com
- Stewart, D. P., Jewell, R. J., & Randolph, M. F. (1994). Design of piled bridge abutments on soft clay for loading from lateral soil movements. *Geotechnique*, 44, 277–296.
- Yamagami, T., Jiang, J.-C., & Ueno, K. (2000). A limit equilibrium stability analysis of slopes with stabilizing piles. In *Slope Stability 2000* (pp. 343–354).
- Zeng, S., & Liang, R. Y. (2002). Stability analysis of drilled shafts reinforced slope. *Soils and Foundations*, 42, 93–102.